Journal of Cancer Research and Experimental Oncology

Volume 5 Number 1, November 2013

ISSN 2141-2243

Academic Journals

ABOUT JCREO

The **Journal of Medical Laboratory and Diagnosis (JMLD)** is published monthly (one volume per year) by Academic Journals.

The **Journal of Cancer Research and Experimental Oncology (JCREO)** is an open access journal that provides rapid publication (monthly) of articles in all areas of the subject such as mammography, chemotherapy, cancer prevention, advances in monoclonal antibody therapy etc.

Submission of Manuscript

Submit manuscripts as e-mail attachment to the Editorial Office at: jcreo@academicjournals.org. A manuscript number will be mailed to the corresponding author shortly after submission.

The Journal of Cancer Research and Experimental Oncology (JCREO) will only accept manuscripts submitted as e-mail attachments.

Please read the **Instructions for Authors** before submitting your manuscript. The manuscript files should be given the last name of the first author.

Instructions for Author

Electronic submission of manuscripts is strongly encouraged, provided that the text, tables, and figures are included in a single Microsoft Word file (preferably in Arial font).

The **cover letter** should include the corresponding author's full address and telephone/fax numbers and should be in an e-mail message sent to the Editor, with the file, whose name should begin with the first author's surname, as an attachment.

Article Types
Three types of manuscripts may be submitted:

Regular articles: These should describe new and carefully confirmed findings, and experimental procedures should be given in sufficient detail for others to verify the work. The length of a full paper should be the minimum required to describe and interpret the work clearly.

Short Communications: A Short Communication is suitable for recording the results of complete small investigations or giving details of new models or hypotheses, innovative methods, techniques or apparatus. The style of main sections need not conform to that of full-length papers. Short communications are 2 to 4 printed pages (about 6 to 12 manuscript pages) in length.

Reviews: Submissions of reviews and perspectives covering topics of current interest are welcome and encouraged. Reviews should be concise and no longer than 4-6 printed pages (about 12 to 18 manuscript pages). Reviews are also peer-reviewed.

Review Process

All manuscripts are reviewed by an editor and members of the Editorial Board or qualified outside reviewers. Authors cannot nominate reviewers. Only reviewers randomly selected from our database with specialization in the subject area will be contacted to evaluate the manuscripts. The process will be blind review.
Decisions will be made as rapidly as possible, and the journal strives to return reviewers' comments to authors as fast as possible. The editorial board will re-review manuscripts that are accepted pending revision. It is the goal of the JPP to publish manuscripts within weeks after submission.

Regular articles

All portions of the manuscript must be typed double-spaced and all pages numbered starting from the title page.

The **Title** should be a brief phrase describing the contents of the paper. The Title Page should include the authors' full names and affiliations, the name of the corresponding author along with phone, fax and E-mail information. Present addresses of authors should appear as a footnote.

The **Abstract** should be informative and completely self-explanatory, briefly present the topic, state the scope of the experiments, indicate significant data, and point out major findings and conclusions. The Abstract should be 100 to 200 words in length. Complete sentences, active verbs, and the third person should be used, and the abstract should be written in the past tense. Standard nomenclature should be used and abbreviations should be avoided. No literature should be cited.
Following the abstract, about 3 to 10 key words that will provide indexing references should be listed.

A list of non-standard **Abbreviations** should be added. In general, non-standard abbreviations should be used only when the full term is very long and used often. Each abbreviation should be spelled out and introduced in parentheses the first time it is used in the text. Only recommended SI units should be used. Authors should use the solidus presentation (mg/ml). Standard abbreviations (such as ATP and DNA) need not be defined.

The **Introduction** should provide a clear statement of the problem, the relevant literature on the subject, and the proposed approach or solution. It should be understandable to colleagues from a broad range of scientific disciplines.

Materials and methods should be complete enough to allow experiments to be reproduced. However, only truly new procedures should be described in detail; previously published procedures should be cited, and important modifications of published procedures should be mentioned briefly. Capitalize trade names and include the manufacturer's name and address. Subheadings should be used. Methods in general use need not be described in detail.

Results should be presented with clarity and precision. The results should be written in the past tense when describing findings in the authors' experiments. Previously published findings should be written in the present tense. Results should be explained, but largely without referring to the literature. Discussion, speculation and detailed interpretation of data should not be included in the Results but should be put into the Discussion section.

The Discussion should interpret the findings in view of the results obtained in this and in past studies on this topic. State the conclusions in a few sentences at the end of the paper. The Results and Discussion sections can include subheadings, and when appropriate, both sections can be combined.

The Acknowledgments of people, grants, funds, etc should be brief.

Tables should be kept to a minimum and be designed to be as simple as possible. Tables are to be typed double-spaced throughout, including headings and footnotes. Each table should be on a separate page, numbered consecutively in Arabic numerals and supplied with a heading and a legend. Tables should be self-explanatory without reference to the text. The details of the methods used in the experiments should preferably be described in the legend instead of in the text. The same data should not be presented in both table and graph form or repeated in the text.

Figure legends should be typed in numerical order on a separate sheet. Graphics should be prepared using applications capable of generating high resolution GIF, TIFF, JPEG or Powerpoint before pasting in the Microsoft Word manuscript file. Tables should be prepared in Microsoft Word. Use Arabic numerals to designate figures and upper case letters for their parts (Figure 1). Begin each legend with a title and include sufficient description so that the figure is understandable without reading the text of the manuscript. Information given in legends should not be repeated in the text.

References: In the text, a reference identified by means of an author‘s name should be followed by the date of the reference in parentheses. When there are more than two authors, only the first author‘s name should be mentioned, followed by ’et al‘. In the event that an author cited has had two or more works published during the same year, the reference, both in the text and in the reference list, should be identified by a lower case letter like ’a‘ and ’b‘ after the date to distinguish the works.

Examples:

Cole (2000), Steddy et al. (2003), (Kelebeni, 1983), (Bane and Jake, 1992), (Chege, 1998; Cohen, 1987a,b;Tristan, 1993,1995), (Kumasi et al., 2001)

References should be listed at the end of the paper in alphabetical order. Articles in preparation or articles submitted for publication, unpublished observations, personal communications, etc. should not be included in the reference list but should only be mentioned in the article text (e.g., A. Kingori, University of Nairobi, Kenya, personal communication). Journal names are abbreviated according to Chemical Abstracts. Authors are fully responsible for the accuracy of the references.

Examples:

Ansell J, Hirsh J, Poller L (2004). The pharmacology and management of the vitamin K antagonists: the Seventh ACCP Conference on Antithrombotic and Thrombolytic. Therapy 126:204-233

Ansell JE, Buttaro ML, Thomas VO (1997). Consensus guidelines for coordinated outpatient oral anti coagulation therapy management. Ann. Pharmacother. 31:604-615

Charnley AK (1992). Mechanisms of fungal pathogenesis in insects with particular reference to locusts. In: Lomer CJ, Prior C (eds), Pharmaceutical Controls of Locusts and Grasshoppers: Proceedings of an international workshop held at Cotonou, Benin. Oxford: CAB International. pp 181-190.

Jake OO (2002). Pharmaceutical Interactions between *Striga hermonthica* (Del.) Benth. and fluorescent rhizosphere bacteria Of *Zea mays*, L. and *Sorghum bicolor* L. Moench for Striga suicidal germination In *Vigna unguiculata*. PhD dissertation, Tehran University, Iran.

Furmaga EM (1993). Pharmacist management of a hyperlipidemia clinic. Am. J. Hosp. Pharm. 50: 91-95

Short Communications

Short Communications are limited to a maximum of two figures and one table. They should present a complete study that is more limited in scope than is found in full-length papers. The items of manuscript preparation listed above apply to Short Communications with the following differences: (1) Abstracts are limited to 100 words; (2) instead of a separate Materials and Methods section, experimental procedures may be incorporated into Figure Legends and Table footnotes; (3) Results and Discussion should be combined into a single section.

Proofs and Reprints: Electronic proofs will be sent (e-mail attachment) to the corresponding author as a PDF file. Page proofs are considered to be the final version of the manuscript. With the exception of typographical or minor clerical errors, no changes will be made in the manuscript at the proof stage.

Fees and Charges: Authors are required to pay a $550 handling fee. Publication of an article in the Journal of Cancer Research and Experimental Oncology (JCREO) is not contingent upon the author's ability to pay the charges. Neither is acceptance to pay the handling fee a guarantee that the paper will be accepted for publication. Authors may still request (in advance) that the editorial office waive some of the handling fee under special circumstances.

Submission of a manuscript implies: that the work described has not been published before (except in the form of an abstract or as part of a published lecture, or thesis) that it is not under consideration for publication elsewhere; that if and when the manuscript is accepted for publication, the authors agree to automatic transfer of the copyright to the publisher.

Journal of Cancer Research and Experimental Oncology

Table of Contents: Volume 5 Number 1 November 2013

ARTICLES

Research Articles

academicJournals

Vol. 5(1), pp. 1-7, November, 2013
DOI: 10.5897/JCREO2013.0101
ISSN 2141-2243 ©2013 Academic Journals
http://www.academicjournals.org/JCREO

Journal of Cancer Research and Experimental Oncology

Full Length Research Paper

Mapping Angiogenic Cells CD31 (*PECAM1*) and CD45 in PCa and BPH Biopsies

Adegun P.T[1]*, Ogundele O.M[2], Falode D.T[3], Taiwo O.J[4], Ajonijebu D.C[5], Omoaghe A.O[5] and Kobomoje O.S[6]

[1]Ekiti State University Teaching Hospital, Ado-Ekiti, Department of Urology, College of Medicine.
[2]Afe Babalola University, College of Medicine and Health Sciences, Department of Anatomy.
[3]Blood and Cancer Centre, American Hospitals and Resorts, Lagos, Nigeria.
[4]Ekiti State University Teaching Hospital, Ado-Ekiti, Department of Histopathology, College of Medicine.
[5]Afe Babalola University, College of Medicine and Health Sciences Department of Physiology, College II.
[6]Afe Babalola University, College of Sciences, Department of Biological Sciences, College.

Accepted 2 October, 2013

Molecular characterization of PCa and BPH using the angiogenic tissue markers CD31 and CD45 to differentiate between the two major types of prostate gland disorders is investigated. 8 clinically characterized biopsies were analyzed at the Histopathology Laboratory of the Ekiti State University Teaching Hospital; the tissue sections were processed for antigen retrieval and were labeled with *anti-CD45* and *anti-CD31* to map the location of angiogenic cells and vascularization in BPH and PCa. The results showed that PCa biopsies expressed embryonic stem cell status of CD31+/CD45+, while BPH showed CD31-/CD45+. This suggests the presence of migrating blood cells (vascularization) in PCa and the absence of such in BPH. It also confirms the role of platelets in endothelial activation that can result to cell proliferation and apoptosis in the prostate gland of either BPH or PCa diagnosed patients.

Key words: CD31, CD45, Prostate, Endothelioma, Vascularization, Angiogenesis

INTRODUCTION

Angiogenesis is a very important factor in the progression of benign tumors and malignancies. As the tumors get vascularized, mapping the angiogenesis markers is an important tool in detection of prostate benign neoplasm progression and malignancy (Ting et al., 2013). Specific protein targeting and labeling are important for this detection. The cluster of differentiations- CD31 and CD45 were selected as the angiogenic tumor markers for PCa as they are important parameters in the determination of micro vessel density within the prostate gland (Li et al., 2013). CD31 (PECAM 1) is a platelet endothelial factor responsible for cell-to-cell adhesion and plays important (Cooper et al., 2002). CD31 can be localized on a wide variety of cells including T-lymphocytes. Of importance is its presence in the endothelial cells and intercellular junctions; this protein functions within a larger family of immunoglobin (Ig's) involved in angiogenesis.

It is also expressed in certain types of tumors especially in the glandular tissue of the prostate (Maeshima et al., 2001). Immunodetection of CD31 can help determine the index of vascularization as in PCa and BPH progression in otherwise what is called tumor angiogenesis or tissue angiogenesis which may be roles in removing aged neutrophils from the body. It is also important in the activation of alpha intergrin receptors required to hold leukocytes to the endothelium caused by inflammation and other fibrous tissue changes within glandular tissue (Gravina et al., 2013). This is also

*Corresponding author. E-mail: ola.ogundele@abuad.edu.ng.

important in the demonstration of prostatic angiomas and angiosacromas (Jin et al., 2013; Tafani et al., 2011). CD45 is a protein tyrosine phosphate (PTP) located in hematopetic cells; the enzymes initiates dephosphorylation of phosphotyrosine residue and are characterized by homologous cyclic domains (Carvalho et al., 2013). The CD45 has several isoform peculiar to specific cell types; *CD45* is a protein expressed in mature lymphocytes that are activated as a form of response to apoptosis; apoptosis not programmed cell death, but physiological cell death in this context (Brennen et al., 2013). This study evaluates prostatic cellular disorders, (BPH and PCa), where CD31 is mapped against CD45 to determine the angiogenesis index in PCa and BPH.

MATERIALS AND METHODS

Tissue processing

BPH and PCa samples (biopsies) were obtained from patients clinically diagnosed and histologically confirmed to have the condition(s) following ethical guidelines approved by the Ekiti State University Teaching Hospital, Ado-Ekiti. The biopsies were fixed in formolcalcium (4BPH and 4Pca) and processed histologically to obtain paraffin wax embedded sections at the Pathology Laboratory of Ekiti State University Teaching Hospital, Ado-Ekiti.

Histology and immunohistochemistry

Tissue sections were processed for routine hematoxylin and eosin following the methods of Zhang et al. (2012) to demonstrate the general morphology of the tissues and vessels in the tissue (small arteries).

CD31/PECAM 1

The following proteins were labeled in the BPH and PCa tissue biopsies; *CD31* in the glandular tissue of the prostate, *CD31* in the muscular part of the prostrate and *CD31* in the endothelium of blood vessels [anti Human-*CD31* monoclonal diluted in Tris buffer saline (TBS) 1:500].

Lymphocytic marker (*CD45+)*

This was demonstrated in the overall prostate tissue (glandular and muscular part) as an indirect measure of lymphocytic cell response at the onset of tumorgenesis (if any; progression of physiological cell death). [*CD45* Anti-human monoclonal diluted in PBS at 1:100]

Procedure

The paraffin wax embedded sections were mounted on a glass slide in preparation for antigen retrieval where the slides were immersed in urea overnight and then placed in a microwave for 45 min to re-activate the antigens and proteins in the tissue sections. Primary antibody treatment involved treating the sections with biotinylated goat serum for one hour following which the sections were transferred to 1% bovine serum albumin (BSA) to block non-specific protein reactions. Secondary treatment involved the use of diluted anti-CD31 and anti-*CD45* on the pre-treated sections for 1 h. The immunopositive reactions were developed using a polymer 3'3' diaminobenzidine tetrachloride (DAB) with colour intensification involving the use of mathenamine silver kit. The sections were counterstained in coomasie-G250 (brilliant blue) and treated in 1% acid alcohol (freshly prepared).

Transformation

Mathenamine silver intensification is used on the immunoperoxidase preparation after the peroxidase/H_20_2/DAB reaction has been carried out to give a brown deposit. The sections were then counterstained in Hematoxylin. The counterstained sections were washed in running tap water, thoroughly rinsed in distilled water, and placed in preheated methenamine silver solution at 60°C for 5 min. Although it could be occasionally longer if the intensification had been carried out at room temperature. In this study, to further increase the clarity, hematoxylin was removed from counterstained nuclei with 1% acid alcohol before the silver intensification was carried out. The composition of the stock solution was 0.125% silver nitrate in 1.5% hexamine. The solution was stored at 4^oC. Prior to use, 2 ml of 5% tetra borate was added to 50 ml of the stock silver solution giving a pH of 8.0, which was then filtered into a coupling jar and protected from sunlight.

RESULTS AND DISCUSSION

The study involves characterization of BPH and PCa biopsies from human prostate by staining the biopsies immunohistochemically using surface antigens for tumor angiogenic cells CD31 and CD45. The nuclei were stained blue following hematoxylin counter stain (Figures 1 to 3). Over the years the controversy of a possible link between BPH and PCa has been extensively discussed; researchers have described the possibility of BPH progressing to PCa. To clarify the essence of the controversy in the first instance, BPH tissue cells will later become tumorgenic or secondly, the presence of symptoms of BPH may predispose to PCa by cellular activation of glandular tissue (Chen et al., 2012).

A major feature peculiar to both BPH and PCa is an increase in the rate of cell proliferation. The clinical manifestations of prostate cancer result from the effects of local growth of the tumor, the spread to regional lymph nodes via the lymphatic system, and the hematogenous dissemination to distant metastatic sites. Although most patients with early-stage prostate cancer are asymptomatic, locally advanced disease can lead to obstructive or irritative voiding symptoms that result from local tumor growth into the urethra or bladder neck, extension into the trigone of the bladder or both making it difficult to differentiate from symptomatic BPH. However, BPH arises as spherical masses of epithelial and stromal elements from the glands lining the proximal prostatic urethra. The ratio of epithelium to smooth muscle in the prostate can vary among individuals, from 1:3 to 4:1.

However, larger prostates may contain more androgen-dependent epithelial elements than smaller glands, which contain a higher proportion of smooth muscle. In either case, the outcome of BPH may be urethral obstruction induced mechanically by epithelial overgrowth and

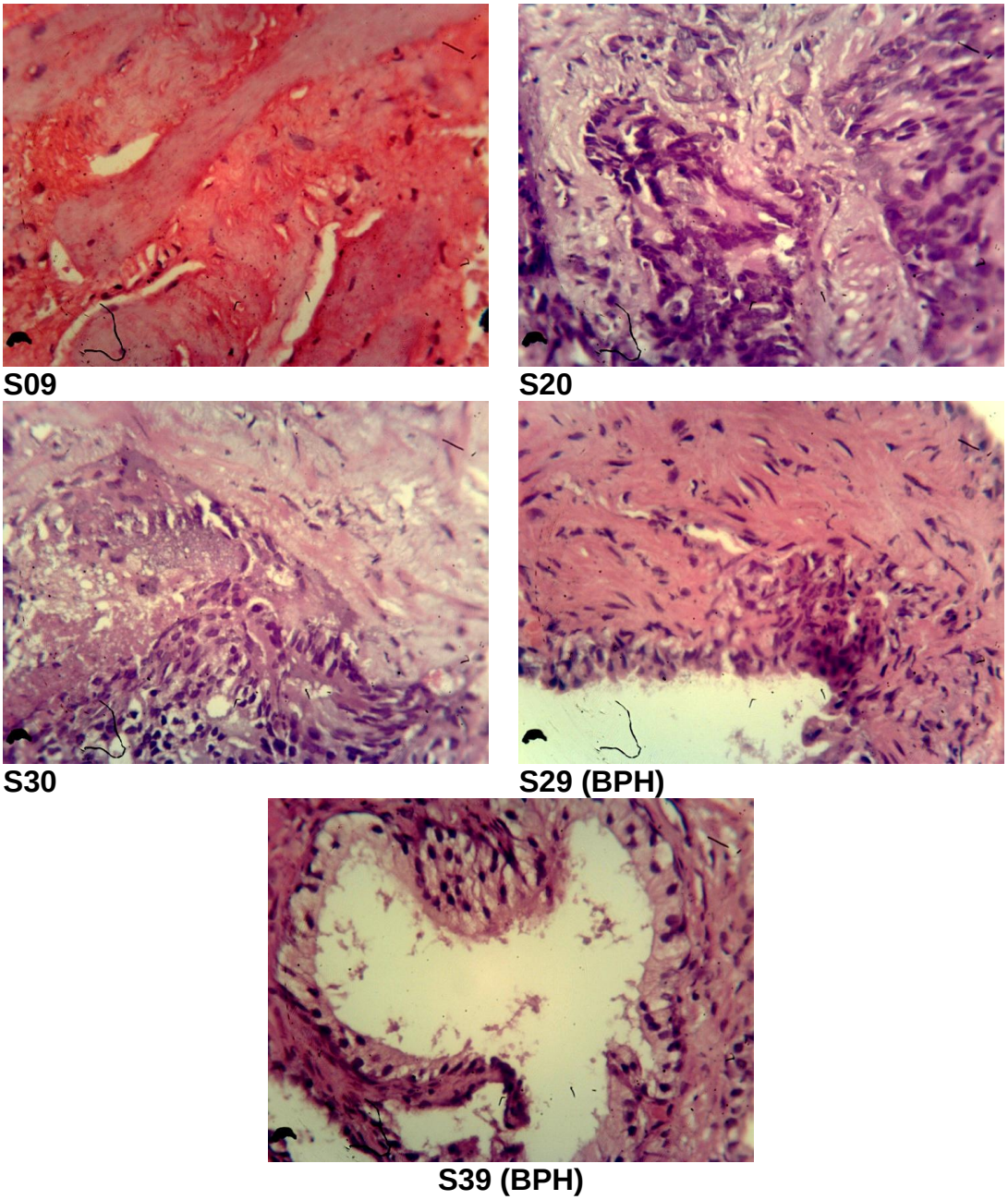

Figure 1. Histological demonstration of the general morphology in human prostate tissue S09, S20 and S30 for PCa while S29 and S39 represent the general morphology of BPH tissues. Cell aggregation can be observed in both PCa and BPH; PCa cell aggregations are located at random in glandular tissue or close to the ductal epithelium, while BPH forms an arranged layered mass of cells in the fibromuscular layer. (Magnification ×400).

dynamically by prostatic smooth muscle contraction, or a combination of the two (Kyprianou et al., 1996). In both cases, increased cell population is resultant while PCa contains cell populations clumped to form a tumor at random locations along the epithelium or glandular tissue, resulting in nodular swellings (Figures 1 and 2). The BPH appears to be a more coordinated proliferative process where cell detachment is not observed and the resultant cell mass have a defined layer like appearance.

A major difference between BPH and PCa is that having acquired the cell mass, the cell aggregations in PCa becomes highly vascularized as seen in the distribution of CD31 (CD31+) in 3 PCa biopsies while in BPH no vascularization is observed (CD31-) (Figure 2).

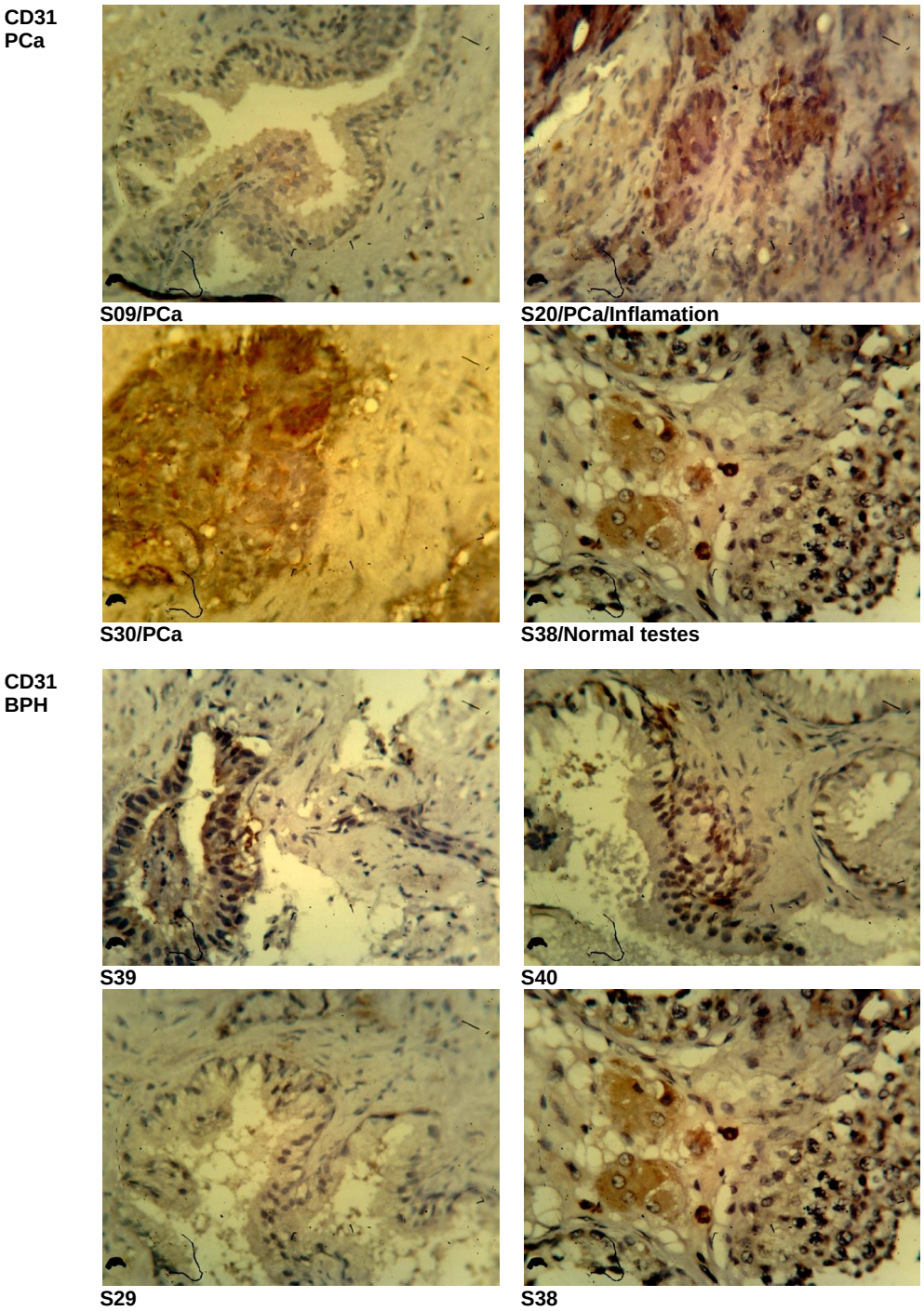

Figure 2. Immunohistochemical demonstration of CD31 in human prostate tissue S09, S20, S30 (PCa). S38 represents the control human testicular tissue. Immunopositivity was observed S30, S09 and S20. Although the level of expression is lower and sparse in S09, this can be accounted for a function of the difference in sites where the tumor cells are localized. While S09 is epithelia, S20 and S30 are glandular and are accessible to vascular supply compared to S09. In the BPH biopsies (S39,S40 and S29), CD31 immunopositivity shows vascularisation of the BPH tissue mass. A feature that seem to accompany cell proliferation. (Magnification ×400).

This is similar to the findings of Wong and Chen (2012) and Chen et al. (2012). The platelet derived factor CD45 are activated as a form of response to apoptosis, the distribution of CD45 was restricted to specific tissue sites

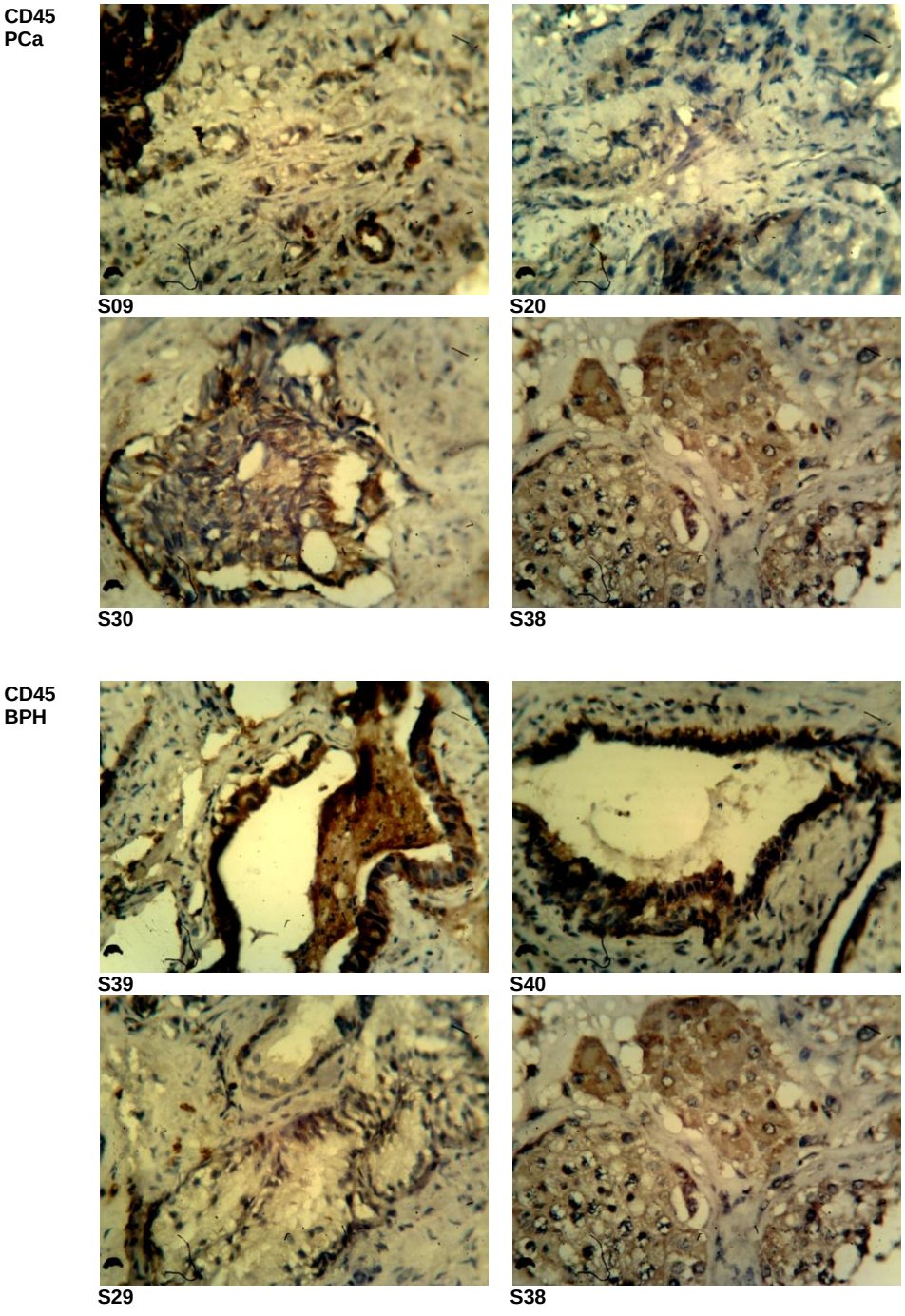

Figure 3. Immunohistochemical demonstration of CD45 in human prostate tissue S09, S20, S30. S38 represents the control human testicular tissue. BPH tissue biopsies S39, S29 and S40). Growing evidence has implicated white adipose tissue as a source of stromal progenitor cell recruited to the tumor microenvironment. S09 (+), S20 (+), S30 (+). In BPH tissues CD45 positivity was observed around the epithelium and was absent in S29 biopsy (Magnification ×400).

within the glandular tissue but negative for the epithelium in PCa biopsies while in BPH, the CD45 was found both around the epithelium of the gland and the fibromuscular layer (Figure 3). CD45 thus seem to be associated with massive cell proliferation (PCa/CD45+ and BPH/CD45+).

This is in agreement with the findings of Morelli et al. (2013) and Jones et al. (2013). Most of the cell death (CD45+) observed were restricted to the surface of the

Table 1. CD31 and CD45 distribution in 4BHP and 4PCa Biopsies following immunohistochemistry using monoclonal antibodies against Human CD31 and CD45.

PCa	*CD31*	*CD45*	BPH	*CD31*	*CD45*
S09	-/+	+	S39	-	+
S20	+	+	S40	-	+
S30	+	+	S29	-	-
S38	+	+	S38	-	+

tumor mass in PCa or tissue mass in BPH. It is characterized by extensive proliferation and inflammation of fibromuscular layer cells which has also been reported to be an important predisposing factor to PCa (Lazar et al., 2012).

In this study PCa recorded CD31+/CD45+ while BPH showed CD31-/CD45+ (Table 1). This result may be useful in predicting the management of carcinoma-*in-situ* as CD31+/CD45+ may suggest progression to PCa. These outcomes may also indicate infiltration of tissue sites by macrophages like eosinophils. There is also a possibility of having the presence of tumor cells from more than one source that is lymphomas and adenocarcinomas. The CD45+ elevated levels in PCa and BPH show activation and aggregation of platelets and according to the studies of Jin et al. (2013), it is a predisposing factor to recurrence of the tumor.

Combined immunodetection of CD31/CD45 also maps the distribution of stimulating proliferating cell populations. Studies on muscles showed that CD31+/CD45- characterized cells constitute about 5 to 6% of cell population in the muscles while CD31-/CD45+ represents the status of 90% of the muscle cells (Figure 3 and Table 1). As a form of response to inflammation, it is possible that CD31+/CD45+ cell population were recruited from elsewhere (Taffani et al., 2011). Tissue sites where CD31+/CD45+ have been identified includes embryonic prostate tissue containing stem cells programmed to form both glandular and muscle tissue of the prostate gland and this is also an evidence of re-expression of embryonic proteins in PCa cells. While the CD31-/CD45+ are characteristic of muscles (90%), it confirms the immune mapping in BPH where the status was CD31-/CD45 (Table 1). CD45 is also peculiar to cells that are capable of active proliferation such as epithelial cells which most of the time undergo exfoliative cytology as part of the routine of the tissue where these cells are localized (Mackern Oberti *et al.,* 2011).

Previous studies already established that CD31 is characteristic of angiogenic cells originating from the bone marrow and such CD31 cells will under defined conditions give rise to endothelial cells and as such it is important to identify cells with increased angiogenic activity (Poveda et al., 2011; Blann et al., 2011). The CD31/CD45 immuno-mapping can also be used as a distinguishing factor for blood cell cancer proper or tumor cells that move within the blood cells (Wong et al., 2012). The role of endothelial cells mapped with CD31 is important in determining the rate of progression of BPH especially those linked with inflammation (Ribeiro et al., 2012). Studies on other endothelial factors like VCAM-1 suggests active chemical interaction in blood vessels (endothelium) to recruit lymphocytic cell lines into the area and induce apoptosis by physiological cell death in the BPH tissue mass or PCa cells (Lawson et al., 2007). In conclusion, the relative distribution of CD31/CD45 is an important molecular marker in determining angiogenesis in PCa progression and also a major tool in distinguishing PCa from BPH.

ACKNOWLEDGEMENT

The authors acknowledge The Laboratory for Biomedical Research and the entire Biomedical Research team of Afe Babalola University, Ado-Ekiti, Nigeria for their assistance.

Conflict of interest statement

The Authors hereby declare there is no conflict of interest associated with this study or any of the procedures and materials used for the purpose of the study

ABBREVIATIONS

PCa; (Prostate Cancer)**, BPH**; (Benign Prostatic Hyperplasia)**, LUTS**; (Lower Urinary Tract Symptoms)**, CD**; (clusters of differentiation).

REFERENCES

Blann AD, Balakrishnan B, Shantsila E, Ryan P, Lip GY (2011). Endothelial progenitor cells and circulating endothelial cells in early prostate cancer: a comparison with plasma vascular markers. Prostate. 71(10):1047-1053.

Brennen WN, Chen S, Denmeade SR, Isaacs JT (2013). Quantification of Mesenchymal Stem Cells (MSCs) at sites of human prostate cancer. Oncotarget. 4(1):106-117.

Carvalho FL, Simons BW, Antonarakis ES, Rasheed Z, Douglas N, Villegas D, Matsui W, Berman DM (2013). Tumorigenic potential

of circulating prostate tumor cells. Oncotarget. 4(3):413-421.
Chen CL, Mahalingam D, Osmulski P, Jadhav RR, Wang CM, Leach RJ, Chang TC, Weitman SD, Kumar AP, Sun L, Gaczynska ME, Thompson IM, Huang TH (2012). Single-cell analysis of circulating tumor cells identifies cumulative expression patterns of EMT-related genes in metastatic prostate cancer. Prostate. 73(8):813-826.
Cooper CR, Bhatia JK, Muenchen HJ, McLean L, Hayasaka S, Taylor J, Poncza PJ, Pienta KJ (2002). The regulation of prostate cancer cell adhesion to human bone marrow endothelial cell monolayers by androgen dihydrotestosterone and cytokines. Clin. Exp. Metastasis. 19(1):25-33.
Gravina GL, Mancini A, Ranieri G, Di Pasquale B, Marampon F, Di Clemente L, Ricevuto E, Festuccia C (2013). Phenotypic characterization of human prostatic stromal cells in primary cultures derived from human tissue samples. J Oncol. 42(6):2116-2122.
Jin R, Sterling JA, Edwards JR, Degraff DJ, Lee C, Park SI, Matusik RJ (2013). Activation of NF-kappa B Signaling Promotes Growth of Prostate Cancer Cells in Bone. PLoS One. 8(4):e60983.
Jones ML, Siddiqui J, Pienta KJ, Getzenberg RH (2013). Circulating fibroblast-like cells in men with metastatic prostate cancer. Prostate. 73(2):176-181.
Kyprianou N, Tu H, Jacobs SC (1996). Apoptotic versus proliferative activities in Human Benign prostatic hyperplesia. Human Pathol. 27(7):668-675.
Lawson DA, Xin L, Lukacs RU, Cheng D, Witte ON (2007). Isolation and functional characterization of murine prostate stem cells. Proc. Nat. Acad. Sci. 104(1):181-186.
Lazar DC, Cho EH, Luttgen MS, Metzner TJ, Uson ML, Torrey M, Gross ME, Kuhn P (2012). Cytometric comparisons between circulating tumor cells from prostate cancer patients and the prostate-tumor-derived LNCaP cell line. Phys Biol. 9(1):016002.
Li O, Tormin A, Sundberg B, Hyllner J, Le Blanc K, Scheding S (2013). Human embryonic stem cell-derived mesenchymal stroma cells (hES-MSCs) engraft in vivo and support hematopoiesis without suppressing immune function: implications for off-the shelf ES-MSC therapies. PLoS One. 8(1):e55319.
Mackern OJP, Breser ML, Nuñez N, Maccioni M, Rodríguez N, Wantia N, Ertl T, Miethke T, Rivero VE (2011). Chemokine response induced by Chlamydia trachomatis in prostate derived CD45+ and CD45- cells. Reproduction. 142(3):427-437.
Maeshima Y, Manfredi M, Reimer C, Holthaus KA, Hopfer H, Chandamuri BR, Kharbanda S, Kalluri R (2001). Identification of the anti-angiogenic site within vascular basement membrane-derived tumstatin. J. Biol. Chem. 276(18):15240-15248.
Morelli A, Comeglio P, Filippi S, Sarchielli E, Vignozzi L, Maneschi E, Cellai I, Gacci M, Lenzi A, Vannelli GB, Maggi M (2013). Mechanism of action of phosphodiesterase type 5 inhibition in metabolic syndrome-associated prostate alterations: an experimental study in the rabbit. Prostate. 73(4):428-441.
Poveda A, Kaye SB, McCormack R, Wang S, Parekh T, Ricci D, Lebedinsky CA, Tercero JC, Zintl P, Monk BJ (2011). Circulating tumor cells predict progression free survival and overall survival in patients with relapsed/recurrent advanced ovarian cancer. Gynecol. Oncol. 122(3):567-572.
Ribeiro R, Monteiro C, Silvestre R, Castela A, Coutinho H, Fraga A, Príncipe P, Lobato C, Costa C, Cordeiro-da-Silva A, Lopes JM, Lopes C, Medeiros R (2012). Human periprostatic white adipose tissue is rich in stromal progenitor cells and a potential source of prostate tumor stroma. Exp. Biol. Med. 237(10):1155-1162.
Tafani M, Di Vito M, Frati A, Pellegrini L, De Santis E, Sette G, Eramo A, Sale P, Mari E, Santoro A, Raco A, Salvati M, De Maria R, Russo MA (2011). Pro-inflammatory gene expression in solid glioblastoma microenvironment and in hypoxic stem cells from human glioblastoma. J. Neuroinflammation. 13:8-32.
Ting H, Deep G, Agarwal R (2013). Molecular Mechanisms of Silibinin-Mediated Cancer Chemoprevention with Major Emphasis on Prostate Cancer. AAPS J. 15(3):707-716.
Wong CK, Namdarian B, Chua J, Chin X, Speirs R, Nguyen T, Fankhauser M, Pedersen J, Costello AJ, Corcoran NM, Hovens CM (2012). Levels of a subpopulation of platelets, but not circulating endothelial cells, predict early treatment failure in prostate cancer patients after prostatectomy. Br. J. Cancer. 107(9):1564-1573.
Zhang ZZ, Gong YY, Shi YH, Zhang W, Qin XH, Wu XW (2012). Valproate promotes survival of retinal ganglion cells in a rat model of optic nerve crush. Neurosci. 224:282-293.

academicJournals

Vol. 5(1), pp. 8-19, November, 2013
DOI: 10.5897/JCREO2013.0102
ISSN 2141-2243 ©2013 Academic Journals
http://www.academicjournals.org/JCREO

Journal of Cancer Research and Experimental Oncology

Full Length Research Paper

Solid-phase total synthesis of cyclic pentapeptide Longicalycinin A, by using 2-chlorotrityl chloride resin

Waqar Ahmad[1,2]*, Farzana Shaheen[2], Yunshan Zhou[1]* and Lijuan Zhang[1]

[1]State Key Laboratory of Chemical Resource Engineering, Institute of Science, Beijing University of Chemical Technology, Beijing 100029, P. R. China.
[2]International Center for Chemical and Biological Sciences, University of Karachi, 75270, Pakistan.

Accepted 3 October, 2013

Naturally isolated cyclic pentapeptide Longicalycinin A, which showed cytotoxicity to Hep G2 cancer cell line with an IC_{50} value 13.52 *μ*g/mL, has been successfully synthesized by solid-phase methodology with Fmoc/*t*-Bu protecting schemes *via* solution-phase macrocyclization. 2-chlorotrityl chloride resin was used as solid support. Solution phase macrocyclization of linear pentapeptide precursor was carried out by two different routes with mild and severe acidic conditions correspondingly and found that percentage yield of Longicalycinin A under mild acidic condition (33%) was better than severe acidic conditions (13.7%). In addition, the cytotoxicity against Dalton's lymphoma ascites (DLA) and Ehrlich's ascites carcinoma (EAC) cell lines with CTC_{50} values were found to be 2.62 and 6.17 *μ*M respectively.

Key words: Longicalycinin A, solid phase synthesis, 2-chlorotrityl chloride, solution-phase macrocyclization, cytotoxicity.

INTRODUCTION

The researchers have paid special attention to the cyclic peptides due to their unique structures and wide spread pharmacological profile, which may solve the problem of wide spread increase of confrontation towards conventional drugs (Poteau and Trinquier, 2005; Tan and Zhou, 2006; Morel et al., 2002; Jennings et al., 2001). Naturally isolated cyclopeptides show various pharmacological activities, such as antitumour (Salvatella et al., 2003; Takeya et al., 1993; Morita et al., 1995), antimalarial (Linington et al., 2007; Isaka et al., 2007), estrogen-like (Itokawa et al., 1995) and tyrosinase inhibitory (Morita et al., 1994).

Solid phase synthesis has many advantages over the classical peptide extraction like the automation of the reaction and the problems of purification and solubilization of the peptide no longer exist since it remains attached to the solid matrix. The most critical feature of solid-phase synthesis is the attachment of substrate to the polymeric resin (Scott, 2009), so the first anchoring unit should be loaded efficiently with polystyrene support and the linkage should be stable enough to tolerate the subsequent chemical transformations and chemical environment. Trityl linker is commonly used in solid-phase peptide synthesis which allows the "protected" compound to be subjected to various chemical manipulations and consequently to afford pure compounds without numerous purification steps (Park et al., 2004; Olsen et al., 2004; Lundquist et al., 2006; Crestey et al., 2008). Additionally, the trityl linker is readily cleaved under mild acidic condition (1% TFA in dichloromethane) owing to the high stability of trityl cations (Rothman et al., 2003).

Cyclic head-to-tail connected peptides can easily be synthesized in good purity using standard procedures

*Corresponding author. E-mail: scholar_waqar@yahoo.com.

and orthogonally protected amino acid residues. However, the cyclization step is critical and depends upon the sequence of peptide, structural constraints, and the resulting ring size. A number of studies have been developed to improve this crucial step and to obtain cyclic peptides in good yield with minimum side reactions (Yang and Morriello, 1999; Li et al., 2002).

A new cyclic pentapeptide Longicalycinin A [*cyclo*-(Gly^1–Phe^2–Pro^3–Tyr^4–Phe^5–)] was isolated from the plant *Dianthus superbus var. longicalycinus* which has been used for treating carcinoma, diuretic and inflammatory diseases showed cytotoxicity to Hep G2 cancer cell line with an IC_{50} value 13.52 μg/mL (Hsieh et al., 2005). By keeping in mind the significance of cytotoxic activity of Longicalycinin A and solid-phase peptide synthesis, this cyclic pentapeptide has been successfully synthesized by solid-phase methodology with Fmoc/*t*-Bu protecting scheme *via* 2-chlorotrityl chloride resin, while macrocyclization was carried out in solution-phase. Solution phase macrocyclization of linear pentapeptide precursor was carried out by two different routes with mild and severe acidic conditions simultaneously and found that percentage yield of Longicalycinin A under mild acidic condition (33%) was better than severe acidic conditions (13.7%). In addition, the cytotoxicity against Dalton's lymphoma ascites (DLA) and Ehrlich's ascites carcinoma (EAC) cell lines with CTC_{50} values were found to be 2.62 and 6.17 μM, respectively.

MATERIALS AND METHODS

All other commercially obtained reagents and solvents were used without further purification. Trifluoroacetic acid (TFA), triisopropylsilane (TIS), Fmoc amino acids and coupling reagents N-hydroxybenzotriazole (HOBt), O-(benzotriazol-1-yl)-*N,N,N′,N′*–tetramethyluranium hexafluoro phosphate (HBTU) were supplied by novabiochem. Solvents like acetonitrile (MeCN), pyridine, piperazine, *N,N*-diisopropylethylamine (DIPEA) and diethyl ether were purchased from Fisher Scientific. 2-chlorotrityl chloride resin (1% DVB, 75~150 µm, 100~200 mesh, sub. rate 1.22 mmol/g) was purchased from Wako. Dichloromethane (DCM), *N, N*-dimethyl formamide (DMF) and methanol (MeOH) were dried according to the Grubb's methods (supporting information).

1HNMR spectra were recorded on Bruker NMR spectrometers operating at 600 MHz. Proton chemical shifts (δ) are reported in ppm. Data are reported as follows: chemical shift (multiplicity [singlet (s), doublet (d), triplet (t), quartet (q) and multiplet (m)], and integration). 13CNMR spectra were recorded on Bruker NMR spectrometers operating at 150 MHz, with complete proton decoupling. NMR data were collected at 25°C. Analytical thin-layer chromatography (TLC) was performed using Silica Gel 60 Å F-254 pre-coated plates (0.25 mm thickness). Visualization was accomplished after spraying with cerric sulphate reagent. High-resolution mass spectra, mass measurements and fast atom bombardment (FAB) mass measurements were recorded on mass spectrometers JEOL JMS HX-110; FAB source using glycerol or thioglycerol as the matrix and cesium iodide (CsI) as internal standard. Optical rotations were measured with a JASCO DIP-360 digital polarimeter at the sodium D line (path length 50 mm). Low-resolution electron impact mass spectra were recorded on a Finnigan MAT-311 with MASPEC Data system. Peak matching, field desorption (FD) and field ionization (FI) were performed on the Finnigan MAT-312 mass spectrometer. Reverse phase LC-908W recycling preparative HPLC was performed on polyamine column with gradient elution using acetonitrile (MeCN) and HPLC grade water (H_2O) (1:2) respectively.

Loading condition for the first amino acid

To the 2-chlorotrityl chloride resin, preswollen in dichloromethane (DCM) (1h), Fmoc-Gly (713.5 mg, 2.4 mmol, 2 equivalents), and *N,N*-diisopropylethylamine (DIPEA) (1.07 mL, 6.10 mmol, 5 equivalents) were added under anhydrous condition. The reaction mixture was stirred under nitrogen atmosphere for 4 h. The reaction was terminated by addition of MeOH/DIPEA (9:1) (10 mL) as scavenger to remove side products. The Fmoc-peptidyl resin **1** was immediately filtered and washed sequentially with DMF (5 mL × 3), DCM (5 mL × 3), and MeOH (5 mL × 3) respectively. The loading of 2 chlorotrityle chloride resin-bound Fmoc glycine in good yields (65 % loading level) has been obtained. After washing, the resin was dried under vacuum for 24 h. The loading efficiency of 2-chlorotrityl chloride resin was determined by loading efficiency procedure (supporting information). The loading degree was found to be 65%, which was determined by UV spectrophotometric analysis (Qin et al., 2003). For the synthesis of the remaining linear pentapeptide, the standard Fmoc protocol was followed (Veber et al., 1984).

Deprotection of Fmoc group

The Fmoc deprotected peptidyl resin was obtained by the addition of 20% piperidine / DMF solution (15 mL) in such a way that the solution just covered the surface of dried Fmoc-peptidyl resin in a two necked round bottom flask (100 mL), with a nitrogen balloon fitted syringe in one neck while the other neck was tightened with a rubber septum and shaked for 30 min, the reaction flask was then placed on a shaker (IKA® -AS130.1) (80 cycles/min). The peptidyl resin was filtered under vacuum, and sequentially washed with 20% piperidine / DMF (10 mL), DMF (5 mL × 5), and finally by DCM (5 mL × 5). The resulting compound was left to dry for 12 h. The Kaiser ninhydrin colorimetric test (supporting information) was performed to confirm the Fmoc deprotection.

Coupling of further amino acids

After loading the first amino acid on polystyrene resin, the resulting peptidyl resin was soaked in DCM (10 mL) for 1 h and then in 2 equivalent concentration of Fmoc-amino acid and treated with coupling reagents [HOBt (324.2 mg, 2.4 mmol, 2 equivalents) and HBTU (910.2 mg, 2.4 mmol, 2 equivalents)] in DIPEA (820 μL, 4 equivalents) for 2 min to form a solution, which was then added to the presoaked (DCM) peptidyl resin and agitated for 4 h at room temperature under nitrogen atmosphere. The reaction was terminated by performing the Kaiser test. After coupling and Fmoc deprotected (20% piperidine/DMF), the anchored resin was filtered and washed with DMF (5 mL × 3) and DCM (5 mL × 3), respectively.

Cytotoxicity

Synthesized Longicalycinin A was subjected to short term *in vitro* cytotoxicity study against Dalton's lymphoma ascites (DLA) (NCRC 101) and Ehrlich's ascites carcinoma (EAC) (NCRC 69) cell lines at 65.5, 32.75, 16.37, 8.18 and 4.09 μg/mL using 5-fluorouracil (5-FU) as reference compound (Kuttan et al., 1985) and three experiments were carried out with each concentration. Activity was assessed by

determining the percentage inhibition of DLA and EAC cells. CTC values were determined by graphical extrapolation method.

The 2-chlorotrityl–Gly^1–Fmoc **1** was subjected to alternate five coupling and five Fmoc deprotection processes, according to general Fmoc deprotection method and general amino acid coupling method as described above, to get compound 2-chlorotrityl–Gly^1–Phe^2–Pro^3–Tyr^4(O*t*-Bu)–Phe^5 **10** (Scheme 1). The progress of each step was confirmed by Kaiser test (Kaiser et al., 1970); the negative test (red color of granular resin) confirmed the coupling, while the positive test (blue color of resin) confirmed the deprotection of Fmoc.

The resulted linear pentapeptide anchored resin **10** was divided in two equal masses and subjected to solution phase macrocyclization through two different routes **A** and **B** (Scheme 2): in one route, first the cleavage step was completed then solution phase macrocyclization was performed and at the end, deprotection of the side chain (O*t*-Bu) was achieved to produce the target molecule Longicalycinin A, while in the other route the cleavage from the solid support and side chain deprotection of O*t*-Bu occurred in a single step followed by solution phase macrocyclization to obtain the target compound (Scheme 2). After cleavage of pentapeptidyl anchored resin, each step was purified by reverse-phase recycling preparative HPLC by using the solvent system of CH_3CN: H_2O, 1:2. A graphical representation of Schemes 1 and 2 is shown in Figure 1.

Macrocyclization Route A

***Synthesis of compound* Gly^1–Phe^2–Pro^3–Tyr^4(O*t*-Bu)–Phe^5 11**

A mixture of 1% trifluoroacetic acid/dichloromethane TFA/DCM was agitated with linear pentapeptide anchored resin **10** for 2 min under nitrogen atmosphere and then filtered under vacuum. The filtrate was treated with a mixture of 10% pyridine/MeOH (50 mL). The same procedure was repeated 10 times and then the filtrate was concentrated in a rotavapor and the crude linear side chain protected pentapeptide Gly^1–Phe^2–Pro^3–Tyr^4(O*t*-Bu)–Phe^5 **11** was purified by HPLC (CH_3CN : H_2O, 1:2) to give one major peak identified on the bases of FAB-MS and ^1H spectrum data as linear side chain protected pentapeptide **11**.

Synthesis of compound [cyclo-(Gly^1-Ph^2-Pro^3-Tyr^4(Ot-Bu)-Phe^5-)] 12

Side chain protected linear pentapeptide **11** (250.7 mg, 0.364 mmol) was dissolved in CH_3CN (360 mL) and treated with HOBT (50.0 mg, 0.364 mmol), HBTU (138.1 mg, 0.364 mmol) and DIPEA (0.38 mL, 2.184 mmol). The solution was maintained at 23°C for 4 days by continuous slow stirring under nitrogen atmosphere and after 4 days, the solution was concentrated in a rotavapor resulting in a yellowish powder which was purified by HPLC (CH_3CN : H_2O, 1:2) to give one major peak identified on the bases of FAB-MS data as a side chain protected cyclic pentapeptide [*cyclo*-(Gly^1-Ph^2-Pro^3-Tyr^4(O*t*-Bu)-Phe^5-)] **12**, (248.3 mg, 99.04 % with respect to compound **11**) (Scheme 2).

Deprotection of compound [cyclo-(Gly^1–Phe^2–Pro^3–Tyr^4(Ot-Bu)–Phe^5)] 12

The side chain deprotection of [*cyclo*-(Gly^1–Phe^2–Pro^3–Tyr^4(O*t*-Bu)–Phe^5)] **12** was achieved by a 2 mL mixture of TFA/H_2O/TIS (95:2.5:2.5). The reaction mixture was kept under stirring for 1 h under nitrogen atmosphere, the solution was concentrated in a rotavapor and the crude cyclic pentapeptide was purified by HPLC (CH_3CN : H_2O 1:2) to give a pure target cyclic pentapeptide Longicalycinin A (81.93 mg, 32.9 % with respect to compound **12**). Furthermore, the recycling of carboxylic acid (e.g. preferably trifluoroacetic acid) trityl ester resins was done by treating the resin with HC1 in CH_2C1_2.

Macrocyclization by Route B

Synthesis of compound Gly^1-Phe^2-Pro^3-Tyr^4-Phe^5 13

A mixture of trifluoroacetic acid/dichloromethane/triisopropylsilane (TFA/DCM/TIPS) (10:9:1) was added to the linear pentapeptide anchored resin 2-chlorotrityl–Gly^1–Phe^2–Pro^3–Tyr^4(O*t*-Bu)–Phe^5 **10** and stirred for 30 min. Under such strong acidic condition cleavage of linear pentapeptide (Gly^1-Phe^2-Pro^3-Tyr^4(O*t*-Bu)-Phe^5) from the 2-chlorotrityl resin as well as side chain deprotection (O*t*-Bu) were carried out in one step. Then this mixture was filtered and washed with a solution of TFA/DCM/TIPS (10:9:1, 20 mL), and DCM (30 mL) after which the filtrate was concentrated in a rotavapor under vacuum and the crude linear pentapeptide was purified by HPLC (CH_3CN : H_2O, 1:2); the HPLC profile showed one major peak which was identified on the bases of FABMS data as linear pentapeptide (Gly^1-Phe^2-Pro^3-Tyr^4-Phe^5) **13** (245.1 mg) (Scheme 2).

Solution-phase macrocyclization of linear pentapeptide Gly^1-Phe^2-Pro^3-Tyr^4 -Phe^5 13

Solution-phase macrocyclization of linear pentapeptide Gly^1-Phe^2-Pro^3-Tyr^4 -Phe^5 **13** was carried out by dissolving 20 mg, 0.0317 mmol of compound **13** in CH_3CN (31.79 mL) and treated with HOBT (4.4 mg, 0.0317 mmol), HBTU (12.0 mg, 0.0317 mmol) and N,N-diisopropylethylamine (DIPEA) (0.038 mL, 0.2184 mmol). The solution was kept at 23°C for 4 days by continuous slow stirring under nitrogen atmosphere and then the solution was concentrated *in vacuo*, resulting in a white yellowish powder and was purified by HPLC (CH_3CN:H_2O, 1:2). The major peak was identified on the bases of FAB-MS, 1H spectrum, 13C spectrum (Table 1), HMBC and HMQC co-relation data as cyclic pentapeptide [*cyclo*-(Gly^1-Phe^2-Pro^3-Tyr^4-Phe^5-)] Longicalycinin A (33.5 mg, 13.7 % with respect to compound **13**).

RESULTS

Characterization of Gly^1–Phe^2–Pro^3–Tyr^4(O*t*-Bu)–Phe^5 11

The physical appearance as an amorphous solid (250.7 mg, 54.05 % with respect to loaded glycine) (scheme 2), R*f* = 0.22 (2:8 MeOH/$CHCl_3$) ; FABMS (+ve) 686.81, 1HNMR (300 MHZ, C_5D_5N, 298 K, major conformation) δ 10.70 (s, OH), δ 8.03 (m, 3H (NH)), δ 7.49 (m, 4H), δ 7.18-7.29 (m, 8H), δ 6.94 (d, 2H), δ 5.15 (t, 1H), δ 5.11 (m, 2H(NH_2)), δ 4.40 (m, 1H), δ 4.14 (s, 2H), δ 3.97 (m, 5H), δ 3.44-3.51 (m, 3H), δ 2.86 (m, 1H), δ 2.32 (m, 2H), δ 2.02 (m, 2H), δ 1.41(s, 9H) (Figure 1B). 13CNMR (C_5D_5N, 125 MHz) δ 174.7, δ 170.5, δ 171.5, δ 170.2, δ 170.1, δ 157.2, δ 137.7, δ 136.4, δ 131.1, δ 128.6, δ 128.3, δ 128.1, δ127.6, δ 125.8, δ 124.8, δ 123.5, δ 116.2, δ 61.1, δ 56.2, δ 55.4, δ 55.7, δ 46.3, δ 44.4, δ 37.6, δ 37.3, δ 37.2, δ 31.7, δ 22.8, δ 11.5 (Figure 2).

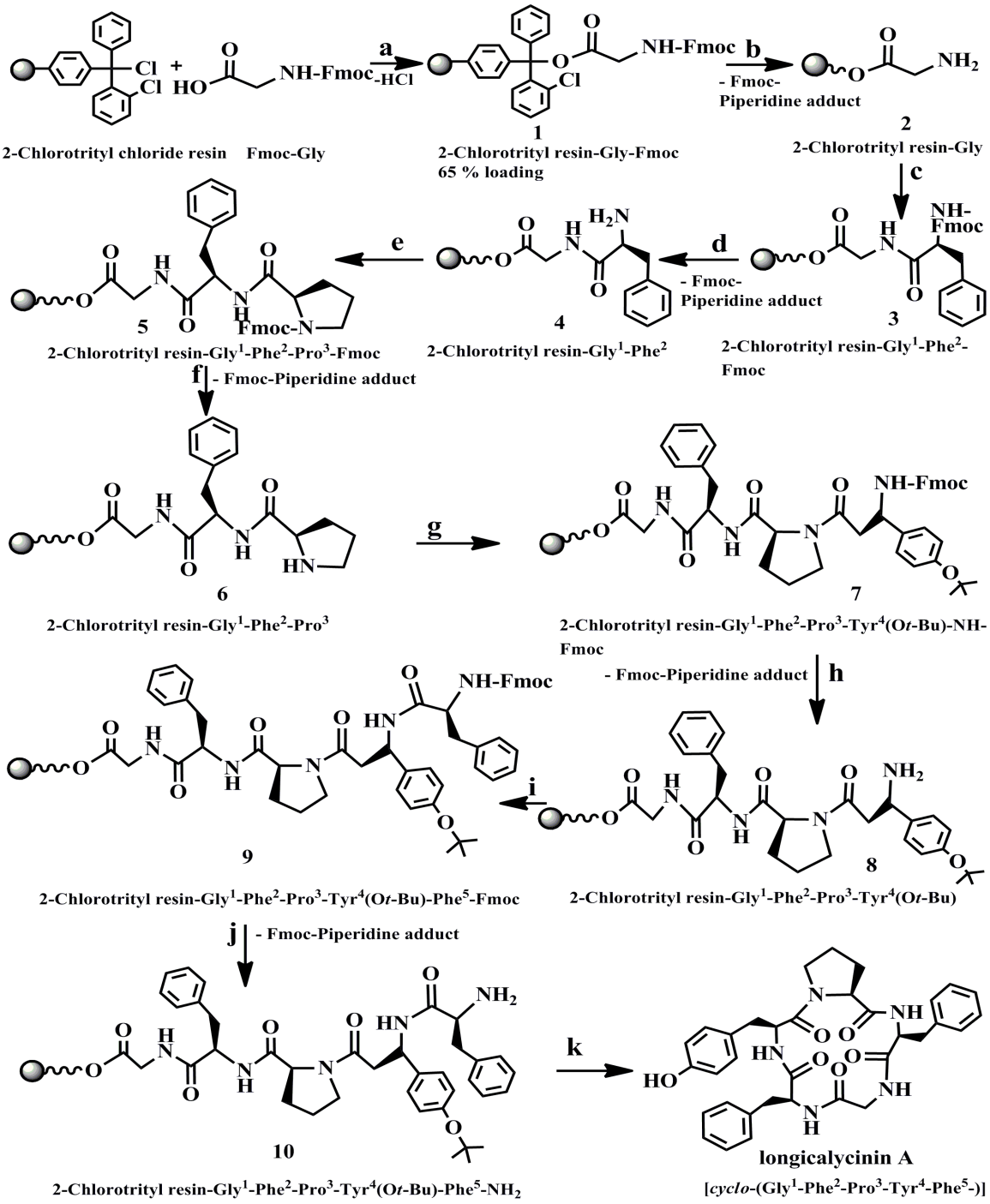

Scheme 1. The Solid-Phase Synthesis of Longicalycinin A *via* 2-chlorotrityl Chloride Linker Reagents.
(**a**) (1) Fmoc-Gly-OH (713.5 mg, 2.4 mmol) (2 equivalents) , (2) DCM (10 mL), (3) DIPEA (1.07 ml, 6.10 mmol) (5 equivalents), Stirring 4h (under nitrogen), (4) MeOH/DIPEA (9:1); (**b**) 20% piperidine/DMF; (**c**) (1) Fmoc-Phe-OH (929.9 mg,2.4mmol) (2 equivalents.), (2) HBTU (910.2 mg, 2.4 mmol) (2 equivalents), (3) HOBT (324.2 mg, 2.4 mmol) (2 equivalents), (4) DIPEA 820 μL (4 equivalents); (**d**) 20% piperidine/DMF; (**e**) (1) Fmoc-Pro-OH (809.7 mg, 2.4 mmol) (2 equivalents), (2) HBTU (910.1 mg, 2.4 mmol) (2 equivalents), (3) HOBT (324.2 mg, 2.4 mmol) (2 equivalents), (4) DIPEA (820 μL) (4 equivalents); (**f**) 20% piperidine/DMF; (**g**) (1) Fmoc-Tyr (*O*t-Bu)-OH (1103.1 mg, 2.4 mmol) (2 equivalents), (2) HBTU (910.2 mg, 2.4 mmol) (2 equivalents), (3) HOBT (324.2 mg, 2.4 mmol) (2 equivalents), (4) DIPEA (820 μL) (4 equivalents); (**h**) 20% piperidine/DMF; (**i**) (1) Fmoc-Phe-OH (929.9 mg, 2.4 mmol) (2 equivalents), (2) HBTU (910.2 mg, 2.4 mmol) (2 equivalents), (3) HOBT (324.2 mg, 2.4 mmol) (2 equivalents), (4) DIPEA (820 μL) (4 equivalents); (**j**) 20% piperidine/DMF; (**k**) (1) TFA/DCM/TIPS (10:9:1) (20 mL), (2) CH_3CN (31.79 mL), (3) HOBT (4.4 mg, 0.0317 mmol), (4) HBTU (12.0 mg, 0.0317 mmol), (5) DIPEA (0.038 mL, 0.2184 mmol).

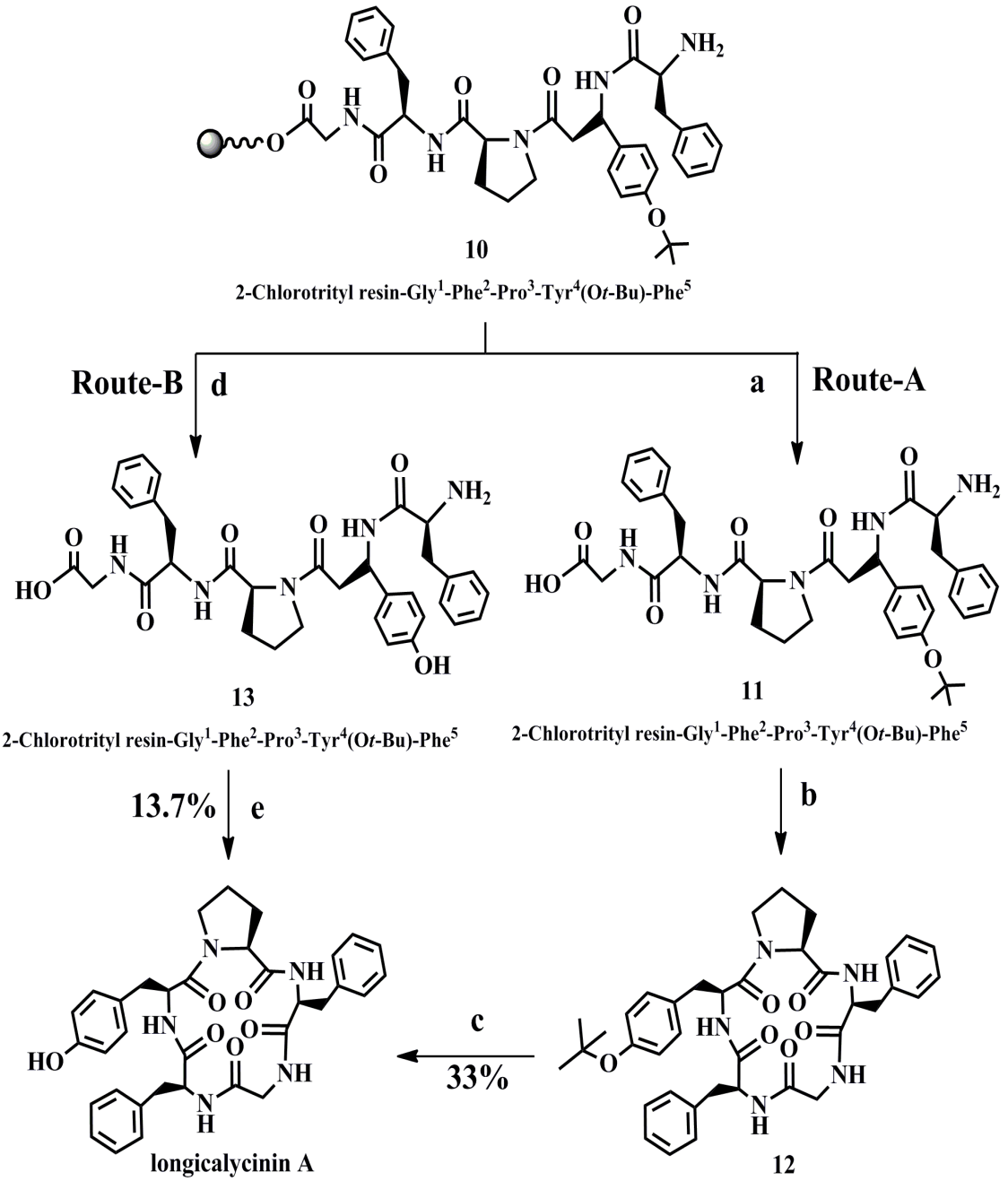

Scheme 2. The Solution-Phase Macrocyclization.
(a) (1) 1% TFA/DCM, (2) 10% pyridine/MeOH ((50 mL); (b) CH_3CN (360 mL), HOBT (50.0 mg, 0.364 mmol), HBTU (138.1 mg, 0.364 mmol), DIPEA (0.38 mL, 2.184 mmol); (c) TFA/H_2O/TIS (95:2.5:2.5); (d) TFA/DCM/TIPS (10:9:1), (e) CH_3CN (31.79 mL), HOBT (4.4 mg, 0.0317 mmol), HBTU (12.0 mg, 0.0317 mmol), (DIPEA) (0.038 mL, 0.2184 mmol).

Characterization of [*cyclo*-(Gly^1-Ph^2-Pro^3-Tyr^4(O*t*-Bu)-Phe^5-)] 12

R*f* = 0.21 (2:8 MeOH/$CHCl_3$) ; FABMS (+ve) 668.79, 1HNMR (300 MHZ, C_5D_5N, 298 K, major conformation) δ 8.0 (m, 2H(NH)), δ 7.40 (m, 4H), δ 7.27-7.29 (m, 6H), δ 7.18 (m, 2H), δ 6.94 (dd, 2H), δ 5.10 (m, 1H), δ 4.92 (m, 1H), δ 4.40 (m, 1H), δ 4.15 (d, 1H), δ 3.95 (m, 1H), δ 3.19-3.44 (m, 4H), δ 2.61-2.86 (m, 2H), δ 2.34 (m, 2H), δ 2.09 (m, 2H), δ 1.41 (s, 9H) (Figure 3). 13CNMR (C_5D_5N, 125 MHz) δ 172.7, δ 172.5, δ 172.3, δ 171.5, δ 170.4, δ 158.0, δ 138.5, δ 137.5, δ 130.0, δ 129.9, δ 129.8, δ 128.7, δ128.6, δ 126.8, δ 123.8, δ 123.8, δ 116.3, δ 61.7, δ 56.4, δ 55.7, δ 55.1, δ 46.9, δ 45.5, δ 38.2, δ 37.6, δ

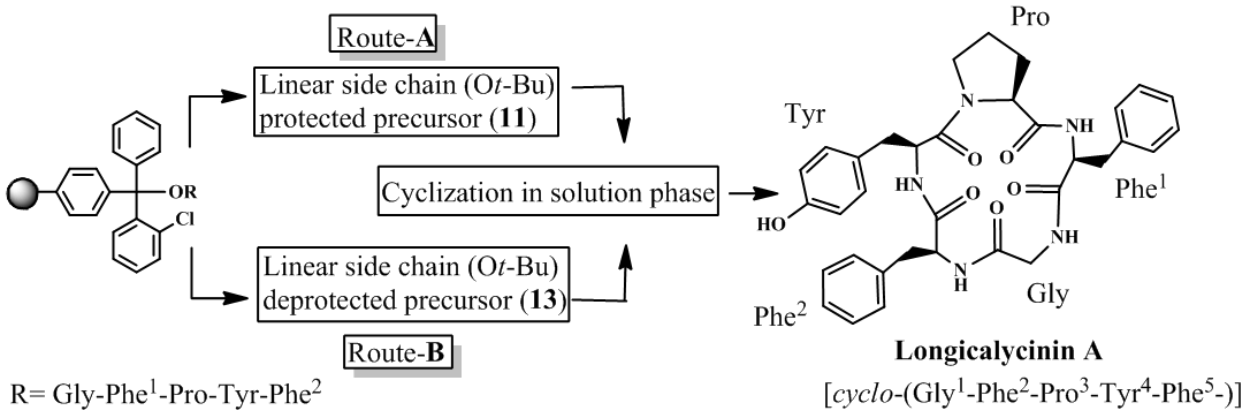

Figure 1A. Graphical abstract of Scheme 1 (The Solid-Phase Synthesis of Longicalycinin A *via* 2-chlorotrityl Chloride Linker) and Scheme 2 (The Solution-Phase Macrocyclization).

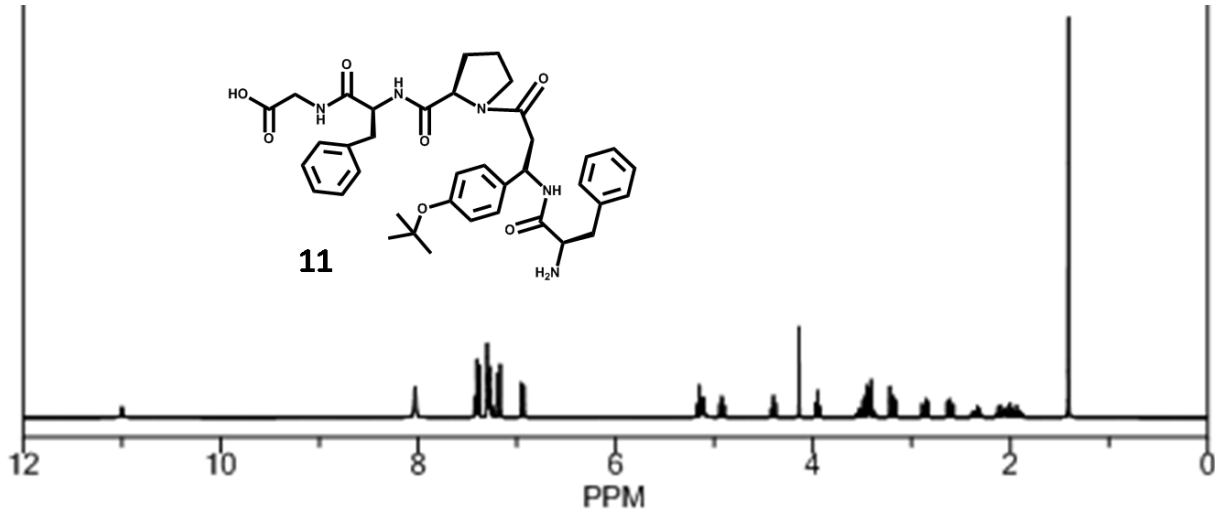

Figure 1B. 1HNMR of compound.

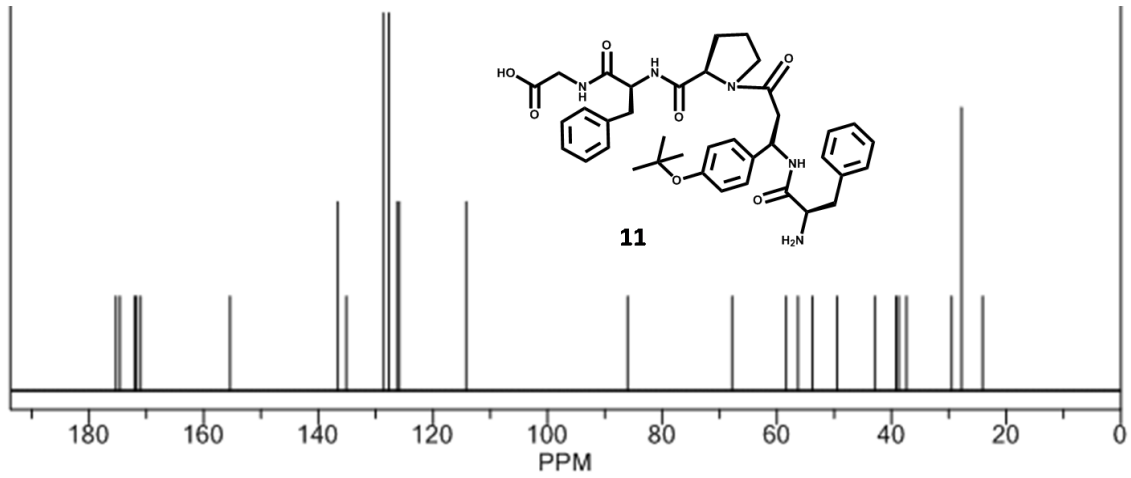

Figure 2. 13CNMR of compound 11

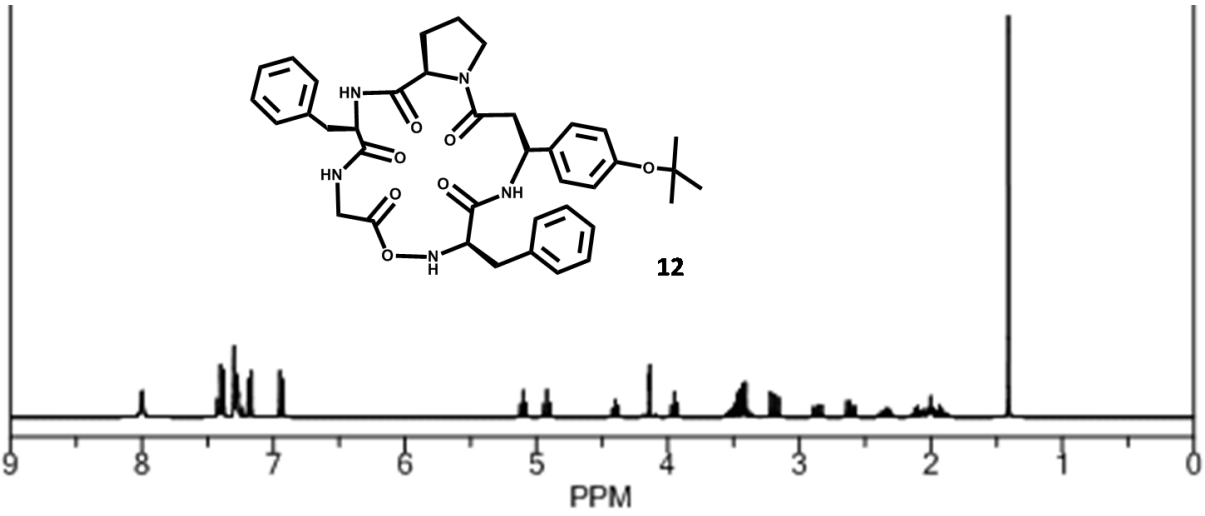

Figure 3. 1HNMR of compound.

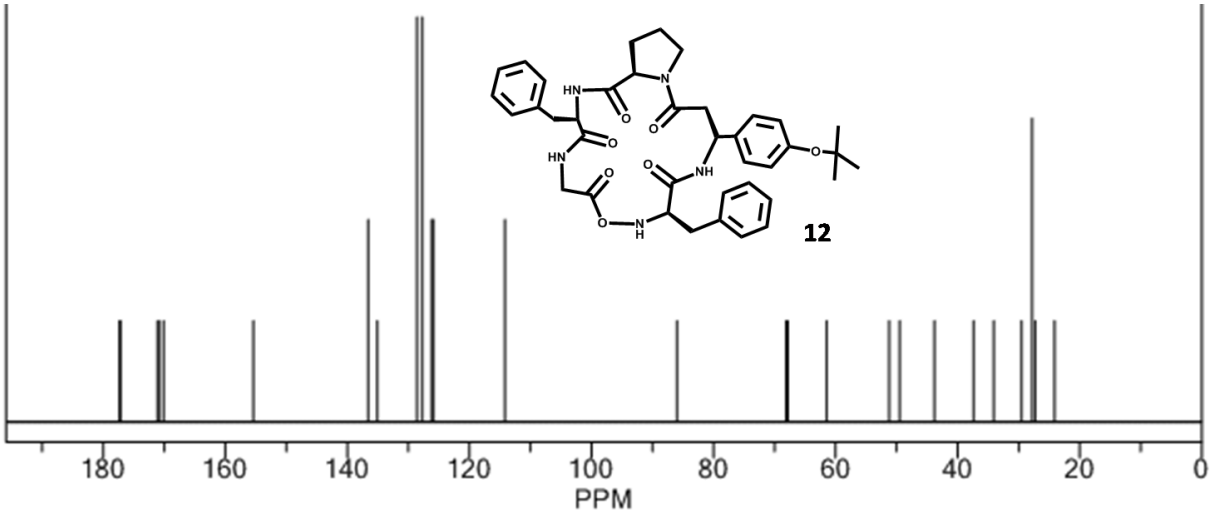

Figure 4. 13CNMR of compound 12.

37.5, δ 31.7, δ 22.9, δ 11.5 (Figure 4).

Characterization of compound Gly[1]-Phe[2]-Pro[3]-Tyr[4]-Phe[5] 13

R*f* = 0.24 (2:8 MeOH/$CHCl_3$) ; FABMS (+ve) 630.7, 1HNMR (300 MHZ, C_5D_5N, 298 K, major conformation) δ 10.86 (s, 1H(OH)), δ 8.03 (s, 3H), δ 7.40 (dd, 4H), δ 7.29 (dd, 4H), δ 7.12 (d, 2H), δ 6.74 (d, 2H), δ 5.35 (s, 1H(OH)), δ 5.17 (m, 2H(NH_2)), δ 5.15 (m, 1H), δ 4.92 (m, 1H), δ 4.40 (m, 1H), δ 4.14 (s, 2H), δ 3.95 (m, 1H), δ 3.44 (m, 4H), δ 2.95 (m, 2H), δ 2.34 (m, 2H), δ 2.02-2.09 (m, 4H) (Figure 5). 13CNMR (C_5D_5N, 125 MHz) δ 175.7, δ 172.5, δ 171.5, δ 170.6, δ 170.5, δ 157.6, δ 137.4, δ 136.7, δ 131.8, δ 129.6, δ 128.5, δ 128.1, δ 127.4, δ 125.6, δ 124.7, δ 123.5, δ 116.3, δ 61.2, δ 56.1, δ 55.6, δ 55.2, δ 46.1, δ 44.6, δ 37.5, δ 37.3, δ 37.2, δ 31.7, δ 22.8, δ 11.5 (Figure 6).

Characterization of [*cyclo*-(Gly[1]-Phe[2]-Pro[3]-Tyr[4]-Phe[5]-)] Longicalycinin A

Longicalycinin A [*cyclo*-(Gly[1]-Phe[2]-Pro[3]-Tyr[4]-Phe[5]-)] physical appeared as a white yellowish amorphous substance. The specific rotation $[\alpha]_D$ was -12° in MeCN solvent. The FAB-MS exhibited $[M+H]^+$ at m/*z* 612. The 1HNMR spectrum (Table 1) of compound [*cyclo*-(Gly[1]-Phe[2]-Pro[3]-Tyr[4]-Phe[5]-)] showed a broad singlet for NH of Phe[5] at δ 9.77. A broad doublet at δ 8.02 (*J* = 9.9 Hz) was due to (NH) proton of Tyr[4], a doublet of one proton at

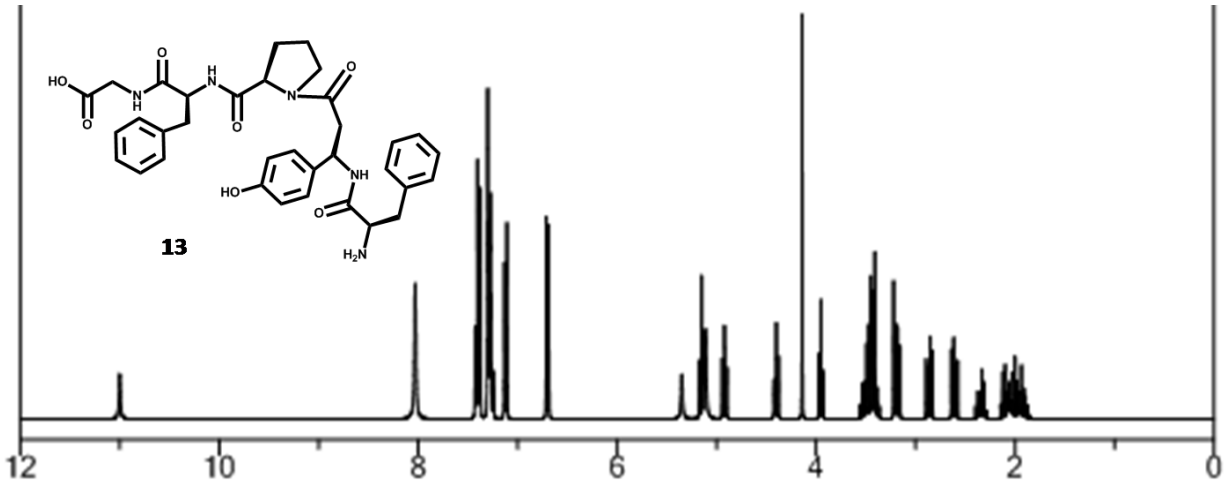

Figure 5. 1HNMR of compound.

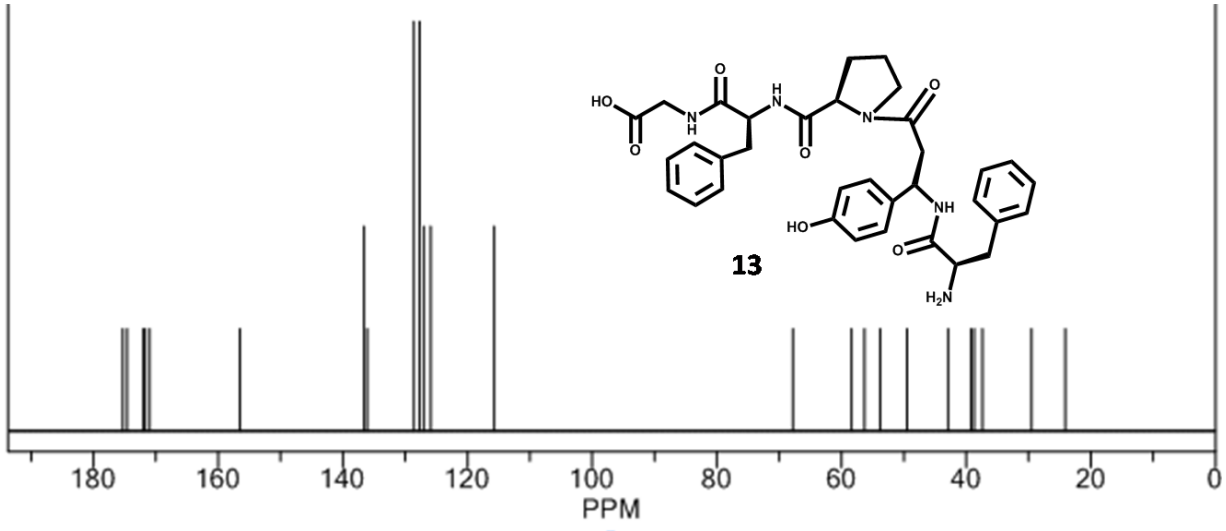

Figure 6. 13CNMR of compound 13.

δ 9.05 (J = 8.2 Hz) was due to NH of Gly[1], a doublet of one proton at δ 7.92 (J = 8.6 Hz) was due to NH of Phe[2] two doublets at δ 7.45 (J = 8.4 Hz) and δ 7.01 (J = 8.4 Hz) were due to aromatic protons of Tyr[4], a triplet at δ 3.70 (J = 9.9 Hz) was due to α proton of Pro[3]. A negative ninhydrin test indicated its cyclic nature. The difference of 13CNMR chemical shifts of Pro[4] ($\Delta\delta$ C_β-C_γ 8.8 ppm) provided evidence that the amide bond in the Pro[3] residue is *cis* (Mergler et al., 1988), (Figures 7, 8).

Cytotoxicity

The results of mean percentage inhibition (mean) and standard deviation (SD) are shown in Tables 2 and 3. Synthesized cyclopeptide exhibited high cytotoxic activity against DLA and EAC cell lines with CTC values of 2.62 and 6.17 μM respectively which in comparison to standard drug 5-fluorouracil (5-FU) (CTC) values were 37.36 and 90.25 μM.

DISCUSSION

To the best of our knowledge the solid-phase syntheses of Longicalycinin A was for the first time carried out using Fmoc/*t*-Bu (Góngora-Benítez et al., 2013) protecting schemes *via* solution-phase Macrocyclization (Jain et al., 2009) Figure 1 A. All the Fmoc-protected amino acids were activated by the HOBt/HBTU in the presence of diisopropylethylamine (DIPEA) before coupling. Immobilization was carried out on 2-chlorotritylchloride resin

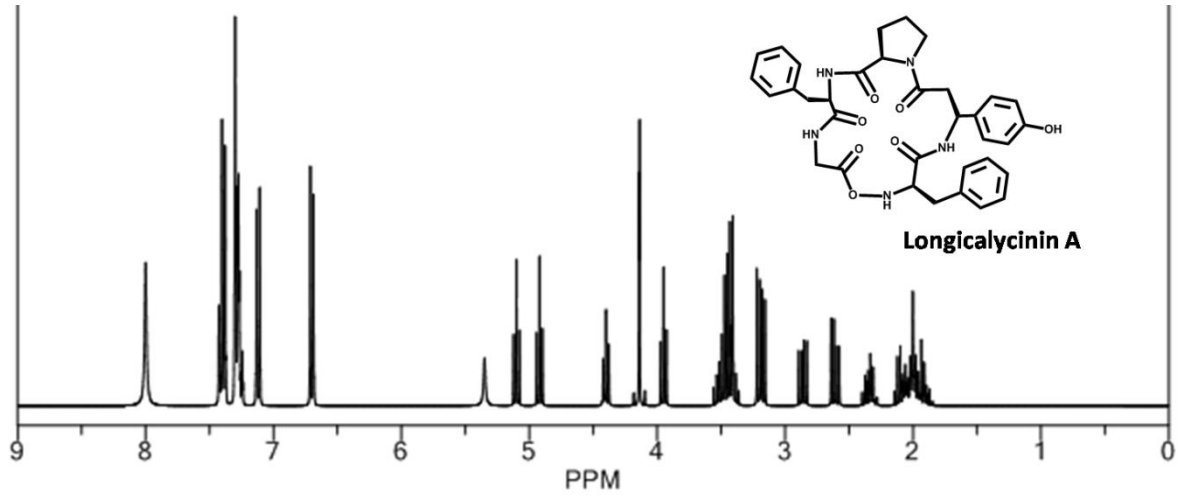

Figure 7. 1HNMR of compound Longicalycinin.

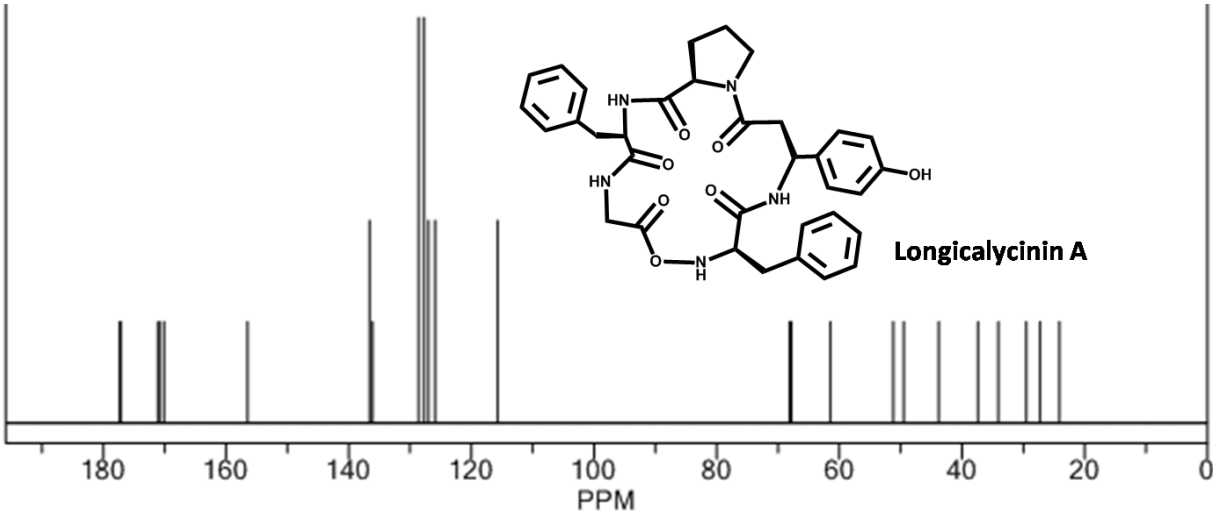

Figure 8. 13HNMR of compound Longicalycinin A.

through the carboxylic acid group of the first Fmoc-Gly *via* 2-chlorotritylchloride linker (Tegge et al., 2010) by DIPEA treatment under anhydrous conditions. The loading step was repeated twice to achieve best loading level. The resulting loading degree (65%) was determined by UV spectrophotometeric analysis (Qin et al., 2003). The resin was subjected to various coupling-deprotection steps to build the linear pentapeptide as the precursor for the cyclic pentapeptide Longicalycinin A. The progress of amino acid coupling was checked through Kaiser's ninhydrin colorimetric test (Kaiser et al., 1970). Fmoc deprotection before each coupling step was achieved by treatment of peptidyl resin with 20% solution of piperidine in DMF.

The linear pentapeptide part of peptidyl resin **10** was cleaved from resin *via* two routes as shown in Scheme 2. In route **A** the cleavage step was achieved by using mild acidic condition to get the side chain protected pentapeptide Gly^1–Phe^2–Pro^3–Tyr^4(O*t*-Bu)–Phe^5 **11** which was subjected to side chain deprotection followed by cyclization in solution phase to get the title compound, while in route **B** the severe acidic condition was used, by which both cleavage of linear pentapeptide from resin and side chain (O*t*-Bu) deprotection of tyrosine unit were done in a single step and then the cleaved side chain deprotected pentapeptide Gly^1-Phe^2-Pro^3-Tyr^4-Phe^5 **13** was subjected to solution phase cyclization to obtain Longicalycinin A. It was found that the percentage yield of Longicalycinin A under mild acidic condition (33%) was better than under severe acidic conditions (13.7%). In

Table 1. ^{1}HNMR and ^{13}CNMR data of Longicalycinin A in Pyridine (C_5D_5N).

Unit		δH, mult. (*J* in Hz)	δC
Gly[1]	C=O		172.3
	NH	7.92 (d, 8.2, 1H)	
	α	4.32 (dd, 2H)	45.5
Phe[2]	C=O		172.5
	NH	9.05 (d, 8.6, 1H)	
	α	5.18 (m, 1H)	55.1
	ß	3.32 (m, 1H)	38.2
		3.21 (m, 1H)	
	Ar	7.15-7.21 (m, 5H)	138.5
			128.6
			129.8
			123.8
Pro[3]	C=O		171.5
	NH		
	α	3.70 (t, 9.9, 1H)	61.7
	ß	1.45 (m, 2H)	31.7
	γ	2.02 (m, 1H)	22.9
		1.88 (m, 1H)	
	δ	3.82 (m, 1H)	46.9
		3.70 (m, H)	
Tyr[4]	C=O		170.4
	NH	8.02 (d, 9.9, 1H)	
	α	4.58 (m,1H)	55.7
	ß	3.08 (m, 1H)	37.6
		3.13 (m, 1H)	
	Ar	7.45 (d, 8.4, 2H)	130.0
		7.01 (d, 8.4, 2H)	126.8
			116.3
			158.0
Phe[5]	C=O		172.7
	NH	9.77 (br s, 1H)	
	α	5.18 (m, 1H)	56.4
	ß	3.40 (m, 2H)	37.5
	Ar	7.18-7.24 (m, 5H)	137.5
			128.7
			129.9
			123.8

route-**A** the tertiary butyl protecting group remained intact with the tyrosine unit which limits the chances of side products resulting in a higher yield in route-**A** as compared to route-**B**, in which deprotected side chain of the tyrosine unit may react with terminal carboxylic acid group of glycine to form an ester linkage. Also in route-B, severe acidic condition may cause the cleavage of amide bonds, and the carboxylic acid group of Gly[1] unit may also react with coupling reagents of HOBT and HBTU (Han et al., 2004).

Each resulting compound was purified by reverse phase recycling preparative HPLC and identified on the basis of Fast Atom Bombardment Mass Spectroscopy (FAB MS) data, 1HNMR spectrum, 13CNMR spectrum and Heteronuclear Multiple Bond Correlation (HMBC) and Heteronuclear Multiple-Quantum Correlation (HMQC). In addition, high cytotoxicity against Dalton's lymphoma ascites (DLA) and Ehrlich's ascites carcinoma (EAC) cell lines with CTC 50 values were found to be 2.62 and 6.17 μM. Recycling reaction may be carried out in organic solvents with high absorption capacity of HCl gas (such as alkylethers, DME, Diglyme, THF or dioxane). The recycling reaction is preferably carried out in the presence of THF or dioxane, most preferred in the presence of dioxane.

Conclusion

A novel, mild and rapid procedure for the loading of 2

Table 2. Cytotoxic activity data of Longicalycinin A for DLA cells.

Conc. (µg/ml)	Sample	Live cells counted	Dead cells counted	% growth inhibition	CTC_{50} (µm)	Mean % growth inhibition± SD	Standard % growth inhibition	Standard CTC_{50} (µm)
	LA1	0	40	100			100	
65.5	LA1	1	39	97.5		96.66±3.81	100	
	LA1	3	37	92.5			100	
	LA2	3	37	92.5			100	
32.75	LA2	3	37	92.5		91.66±1.44	100	
	LA2	4	36	90.0			100	
	LA3	8	32	80.0			75.0	
16.37	LA3	7	33	82.5	2.62	80.83±1.44	75.0	37.36
	LA3	8	32	80.0			75.0	
	LA4	12	28	70.0			65.0	
8.18	LA4	12	28	70.0		70.0±0.00	65.0	
	LA4	12	28	70.0			65.0	
	LA5	25	15	37.5			42.5	
4.09	LA5	26	14	40.0		39.16±1.44	42.5	
	LA5	26	14	40.0			42.5	

LA = Longicalycinine A, SD = Standard deviation, DLA = Dalton's lymphoma ascites, CTC = Common Toxicity Criteria.

Table 3. Cytotoxic activity data of Longicalycinin A for EAC cells.

Conc. (µg/ml)	Sample	Live cells counted	Dead cells counted	% growth inhibition	CTC_{50} (µm)	Mean % growth inhibition± SD	Standard % growth inhibition	Standard CTC_{50} (µm)
	LA6	0	30	100			100	
65.5	LA6	0	30	100		98.86±1.96	100	
	LA6	1	29	96.66			100	
	LA7	2	28	93.3			100	
32.75	LA7	2	28	93.3		93.3±0.00	100	
	LA7	2	28	93.3			100	
	LA8	10	20	66.6			63.3	
16.37	LA8	9	21	70.0	6.17	68.8±1.96	63.3	90.25
	LA8	9	21	70.0			63.3	
	LA9	16	14	46.6			36.6	
8.18	LA9	16	14	46.6		46.6±0.00	36.6	
	LA9	16	14	46.6			36.6	
	LA10	21	9	30.0			23.3	
4.09	LA10	22	9	30.0		31.0±1.73	23.3	
	LA10	20	10	33.3			23.3	

LA = Longicalycinine A, SD = Standard deviation, EAC = Ehrlich Ascites Carcinoma, CTC = Common Toxicity Criteria.

chlorotrityle chloride resin-bound Fmoc glycine in good yields (65 % loading level) has been developed, which will be useful for the solid-phase preparation of polypeptides containing glycine moiety in their structure. The resin recycling capability has been demonstrated using this protocol and the proposed reaction intermediates have been identified by performing the corresponding reactions in solution. The substitution level on the 2-chlorotrityl resin with Fmoc glycine was better and 0.73 mmol/g of amino acid was loaded resulting in a reasonable yield of the target peptide from route **A** (33%) by using mild acidic conditions, and route **B** (13.7%) with severe acidic condition, respectively. In route-**A** the tertiary butyl protecting group remained intact with tyrosine unit which limits the chances of side products thus resulting in a higher yield in route-**A** as compared to route-**B**. Synthesized cyclopeptide exhibited high cytotoxic activity against DLA and EAC cell lines with CTC values of 2.62 and 6.17 μM respectively, in comparison to standard drug 5-fluorouracil (5-FU) (CTC values – 37.36 and 90.25 μM). In future, Longicalycinin A will be prepared by using 4-Sulfamylbutyryl AM resin for comparative yield.

ACKNOWLEDGMENTS

The toxicity study by Sarfaraz Ahmad, International Center for Chemical and Biological Sciences, University of Karachi, Pakistan and financial support from the Higher Education Commission of Pakistan are highly acknowledged.

REFERENCES

Crestey F, Ottesen LK, Jaroszewski JW, Franzyk H (2008). Efficient loading of primary alcohols onto a solid phase using a trityl bromide linker. Tetrahedron Lett. 49:5890-5893.

Han SY, Kim YA (2004). Recent development of peptide coupling reagents in organic synthesis. Tetrahedron. 60:2447-2467.

Hsieh PW, Chang FR, Wu CC, Li CM, Wu KY (2005). Longicalycinin A, a new cytotoxic cyclic peptide from *Dianthus superbus var. longicalycinus* (MAXIM.) WILL. Chem. Pharm. Bull. 53:336-338.

Isaka M, Palasarn S, Lapanun S, Sriklung K (2007). Paecilodepsipeptide A, an antimalarial and antitumor cyclohexadepsipeptide from the insect pathogenic fungus *Paecilomyces cinnamomeus* BCC 9616. J. Nat. Prod. 70:675-678.

Itokawa H, Yun Y, Morita H, Takeya K, Yamada K (1995). Estrogen-like activity of cyclic peptides from *Vaccaria segetalis* extracts. Planta Med. 61:561-562.

Jain RK, Tsou LK, Hamilton AD (2009). Combined solid/solution phase synthesis of large surface area scaffolds derived from aminomethylbenzoates. Tetrahedron Lett. 50:2787-2789.

Jennings CV, West J, Waine C, Craik DJ, Anderson MA (2001). Biosynthesis and insecticidal properties of plant cyclotides: the cyclic knotted proteins from *Oldenlandia affinis*. Proc. Natl. Acad. Sci. 98:10614-10619.

Kaiser E, Colescott RL, Bossinger CD, Cook PI (1970). Color test for detection of free terminal amino groups in the solid-phase synthesis of peptides. Anal. Biochem. 34:595-598.

Kuttan R, Bhanumathy P, Nirmala K, George MC (1985). Potential anticancer activity of turmeric (*Curcuma longa*). Cancer Lett. 29:197-202.

Li P, Roller PP, Xu J (2002). Current synthetic approaches to peptide and peptidomimetic Cyclization. Curr. Org. Chem. 6:411-440.

Linington RG, Gonzalez J, Urena LD, Romero LI, Ortega-Barría E, Gerwick WH (2007). Venturamides A and B: antimalarial constituents of the panamanian marine *Cyanobacterium oscillatoria* sp. J. Nat. Prod. 70:397-401.

Lundquist JT, Satterfield AD, Pelletier JC (2006). Mild and adaptable silver triflate-assisted method for trityl protection of alcohols in solution with solid-phase loading applications. Org. Lett. 8:3915-3918.

Mergler M, Tanner R, Gosteli J, Grogg P (1988). Peptide synthesis by a combination of solid-phase and solution methods I: A new very acid-labile anchor group for the solid phase synthesis of fully protected fragments. Tetrahedron Lett. 29:4005-4008.

Morel AF, Araujo CA, da Silva UF, Hoelzel SC, Zachia R, Bastos NR (2002). Antibacterial cyclopeptide alkaloids from the bark of *Condalia buxifolia*. Phytochem. 61:561-566.

Morita H, Kayashita T, Kobata H, Gonda A, Takeya K, Itokawa H (1994). Pseudostellarins A-C, new tyrosinase inhibitory cyclic peptides from *Pseudostellaria heterophylla*. Tetrahedron. 50:6797-6804.

Morita H, Nagashima S, Takeya K, Itokawa H (1995). Solution forms of antitumor cyclic pentapeptides with 3,4-dichlorinated proline residues, astins A and C, from *Aster tataricus*. Chem. Pharm. Bull. 43:1395-1397.

Olsen CA, Witt M, Jaroszewski JW**,** Franzyk HJ (2004). Solid-phase synthesis of rigid acylpolyamines using temporary N-4,4'-dimethoxytrityl protection in the presence of trityl linkers. J. Org. Chem. 69:6149-6152.

Park JG, Langenwalter KJ, Weinbaum CA, Casey PJ, Pang YP (2004). Improved loading and cleavage methods for solid-phase synthesis using chlorotrityl resins: synthesis and testing of a library of 144 discrete chemicals as potential farnesyltransferase inhibitors. J. Comb. Chem. 6:407-413.

Poteau R, Trinquier G (2005). All-cis cyclic peptides. J. Am. Chem. Soc. 127:3875-13889.

Qin C, Bu X, Wu X, Guo Z (2003). A chemical approach to generate molecular diversity based on the scaffold of cyclic decapeptide antibiotic tyrocidine A. J. Comb. Chem. 5:353-355.

Rothman DM, Vazquez ME, Vogel EM, Imperiali B (2003). Caged phospho-amino acid building blocks for solid-phase peptide synthesis. J. Org. Chem. 68:6795-6798.

Salvatella X, Caba JM, Albericio F, Giralt E (2003). Solution structure of the antitumor candidate trunkamide A by 2D NMR and restrained simulated annealing methods. J. Org. Chem. 68:211-215.

Scott PJH (2009). Linker strategies in solid-phase organic synthesis, Wiley & Sons Ltd, Chichester.

Tan N, Zhou J (2006). Plant cyclopeptides. Chem. Rev. 106:840-895.

Takeya K, Yamamiya T, Morita H, Itokawa H (1993). Two antitumour bicyclic hexapeptides from *Rubia cordifolia*. Phytochem. 33:613-615.

Tegge W, Bonafe CFS, Teichmann A, Erick C (2010). Synthesis of peptides from α- and β-tubulin containing glutamic acid side-chain linked oligo-glu with defined length. Int. J. Pept. 1:1-10.

Veber DF, Saperstein R, Nutt RF, Freidinger RM, Brady SF, Curley P, Perlow DS, Paleveda WJ, Colton CD, Zacchei AG, Tocco DJ, Hoff DR, Vandlen RL, Gerich JE, Hall L, Mandarino L, Cordes EH, Anderson PS, Hirschmann R (1984). A super active cyclic hexapeptide analog of somatostatin. Life Sci. 34:1371-1378.

Yang L, Morriello G (1999). Solid phase synthesis of “head-to-tail” cyclic peptides using a sulfonamide ‘safety-catch’ linker: the cleavage by cyclization approach. Tetrahedron Lett. 40:8197-8200.

UPCOMING CONFERENCES

International Conference on Pharmacy and Pharmacology, Bangkok, Thailand, 24 Dec 2013

17th World Congress of Basic and Clinical Pharmacology, Cape Town, South Africa, 13 Jul 2014

Conferences and Advert

March 2014
3rd International Conference on Medical Information and Bioengineering, Penang, Malaysia, 10 Mar 2014

May 2014
2nd Annual International Conference on Health & Medical Sciences, Athens, Greece, 5 May 2014

Journal of Cancer Research and Experimental Oncology

Related Journals Published by Academic Journals

- International Journal of Medicine and Medical Sciences
- Journal of Medicinal Plant Research
- African Journal of Pharmacy and Pharmacology
- Journal of Clinical Medicine and Research
- Clinical Reviews and Opinions
- Medical Practice and Reviews

academicJournals